Title
Exchange processes of volatile organic compounds above a tropical rain forest: Implications for modeling tropospheric chemistry above dense vegetation

Journal
Journal of Geophysical Research, 109(D18)

ISSN
0148-0227

Authors
Karl, Thomas
Potosnak, Mark
Guenther, Alex
et al.

Publication Date
2004

DOI
10.1029/2004jd004738

Exchange processes of volatile organic compounds above a tropical rain forest: Implications for modeling tropospheric chemistry above dense vegetation

Thomas Karl, Mark Potosnak,[1] and Alex Guenther
Atmospheric Chemistry Division, National Center for Atmospheric Research, Boulder, Colorado, USA

Deborah Clark
Department of Biology, University of Missouri at St. Louis, St. Louis, Missouri, USA

John Walker, Jeffrey D. Herrick, and Chris Geron
National Risk Management Research Laboratory, U.S. Environmental Protection Agency, Research Triangle Park, North Carolina, USA

Received 5 March 2004; revised 24 June 2004; accepted 12 July 2004; published 23 September 2004.

[1] Disjunct eddy covariance in conjunction with continuous in-canopy gradient measurements allowed for the first time to quantify the fine-scale source and sink distribution of some of the most abundant biogenic (isoprene, monoterpenes, methanol, acetaldehyde, and acetone) and photooxidized (MVK+MAC, acetone, acetaldehyde, acetic, and formic acid) VOCs in an old growth tropical rain forest. Our measurements revealed substantial isoprene emissions (up to 2.50 mg m^{-2} h^{-1}) and light-dependent monoterpene emissions (up to 0.33 mg m^{-2} h^{-1}) at the peak of the dry season (April and May 2003). Oxygenated species such as methanol, acetone, and acetaldehyde were typically emitted during daytime with net fluxes up to 0.50, 0.36, and 0.20 mg m^{-2} h^{-1}, respectively. When generalized for tropical rain forests, these fluxes would add up to a total emission of 36, 16, 19, 106, and 7.2 Tg/yr for methanol, acetaldehyde, acetone, isoprene, and monoterpenes, respectively. During nighttime we observed strong sinks for oxygenated and nitrogen-containing compounds such as methanol, acetone, acetaldehyde, MVK+MAC, and acetonitrile with deposition velocities close to the aerodynamic limit. This suggests that the canopy resistance (R_c) is very small and not the rate-limiting step for the nighttime deposition of many VOCs. Our measured mean dry deposition velocities of methanol, acetone, acetaldehyde, MVK+MAC, and acetonitrile were a factor 10–20 higher than estimated from traditional deposition models. If our measurements are generalized, this could have important implications for the redistribution of VOCs in atmospheric chemistry models. Our observations indicate that the current understanding of reactive carbon exchange can only be seen as a first-order approximation. *INDEX TERMS:* 0315 Atmospheric Composition and Structure: Biosphere/atmosphere interactions; 0322 Atmospheric Composition and Structure: Constituent sources and sinks; 0330 Atmospheric Composition and Structure: Geochemical cycles; 0365 Atmospheric Composition and Structure: Troposphere—composition and chemistry; *KEYWORDS:* VOC, flux, PTRMS

Citation: Karl, T., M. Potosnak, A. Guenther, D. Clark, J. Walker, J. D. Herrick, and C. Geron (2004), Exchange processes of volatile organic compounds above a tropical rain forest: Implications for modeling tropospheric chemistry above dense vegetation, *J. Geophys. Res.*, *109*, D18306, doi:10.1029/2004JD004738.

1. Introduction

[2] Predicting the role of the biosphere in the behavior of the Earth system and understanding the interaction between ecosystems and the atmosphere is becoming an increasingly important part of atmospheric science. Historically volatile organic compounds (VOCs) have been recognized as a central part in atmospheric chemistry [*Trainer et al.*, 1987]. Oxygenated compounds, such as acetone, can also influence the HO_x cycle in the upper troposphere [*McKeen et al.*, 1997] or can be converted to acetylperoxy radicals by atmospheric oxidation and lead to formation of peroxyacetic nitric anhydride (PAN) type compounds, which act as relatively long-lived temporary reservoirs for nitrogen oxides (NO_x) [*Roberts et al.*, 2002]. As interest in devel-

[1] Now at Desert Research Institute, Reno, Nevada, USA.

0148-0227/04/2004JD004738

opment of Earth system models is rapidly growing, it is becoming clear that VOCs are not only an intrinsic part of the carbon cycle but can also have profound ramifications on the global climate system. *Collins et al.* [2002], for example, showed that the flux of reactive carbon into the atmosphere and its associated effects on global HO distributions can have a significant impact on the lifetimes of important greenhouse gases and the abundance of O_3. *Andreae and Crutzen* [1997] argued that emissions of VOCs could exert additional control over cloud development and precipitation by influencing formation, growth and hygroscopic properties of cloud condensation nuclei (CCN), which in turn could have important feedbacks on evapotranspiration and the hydrological cycle [*Barth et al.*, 2004].

[3] Future land use change is expected to have the most significant impact in the tropics, although some global climate models predict ecosystem collapse in the Amazon basin due to warming and drying in this region [*Cox et al.*, 2000]. Considering the importance of tropical ecosystems on atmospheric processes [*Crutzen et al.*, 2000], available data on the exchange of reactive carbon in these regions are still very scarce.

[4] Classical approaches in ecophysiology, which involve mechanistic studies over the controls of trace gas exchange at the leaf and branch level [*Harley et al.*, 1997; *Schnitzler et al.*, 2002], are challenged by the high species diversity in tropical ecosystems [*Harley et al.*, 2004]. There is also growing evidence that additional processes, such as disturbance/wounding [*Litvak et al.*, 1999; *Fall et al.*, 1999] and various microorganisms feeding on VOCs, e.g., isoprene [*Cleveland and Yavitt*, 1997], can potentially influence the exchange of reactive carbon. In recent years, canopy crane sites have made it possible to access plant communities at different heights, allowing studies in various parts of the canopy [*Ozanne et al.*, 2003]. Despite this progress, the biodiversity and the complex three-dimensional structure of tropical canopies make it extremely difficult to extrapolate exchange processes only based on leaf and branch level observations in any representative manner. In order to obtain meaningful results at the ecosystem level, quantification of the overall exchange processes also needs to be based on micrometeorological techniques and whole canopy measurements. Following recent advances in measuring canopy scale VOC fluxes by indirect and direct methods [*Schade and Goldstein*, 2001; *Karl et al.*, 2001, 2002a, 2003; *Baker et al.*, 2001; *Rinne et al.*, 2002; *Warneke et al.*, 2002], we deployed a proton-transfer-reaction mass spectrometer for disjunct eddy covariance and in-canopy gradient measurements in an old-growth lowland rain forest in Costa Rica during the drier season in 2003. Our measurements show a complex behavior of emission and deposition of some of the most abundant VOCs within and above the canopy and suggest that our current understanding on their chemical and physical cycling is still in its infancy.

2. Site Description and Experimental Details

[5] The La Selva Biological Station (10.43 N, 83.93 W, 80–150 m a.s.l.) is situated in the lowland tropical wet forests of the canton Sarapiqui, province of Heredia, Costa Rica. The tower is surrounded by old-growth tropical wet forest dominated by trees of the canopy species *Pentaclethra macroloba* (~34% of total forest basal area [*Clark and Clark*, 2000]). The landscape-scale median canopy height is 23 m [*Clark et al.*, 1996], with some emergent trees exceeding 50 m (D. B. Clark, unpublished data). Surface winds during this study were dominantly between SSE and WSW, a distribution similar to that previously found at this site by *Loescher et al.* [2004]. The mean wind speed was 2 m/s; the wind speed typically peaked in the afternoon around 1500 local time at ca. 2–4 m/s and stayed above 1.5 m/s during most nights. The maximum wind speed we observed was 5 m/s. Half-hour mean temperatures during our study period ranged between 24 and 32°C. The 2003 dry season (January–March) was characterized by remarkably little precipitation with drought-like conditions toward the end, caused by changes in general atmospheric circulation due to an ENSO year. At the start of the experiment (April 2, 2003) the VOC analysis equipment (1 modified PTR-MS, Ionicon, Austria; 2 gas chromatographs: Shimadzu Inst., Kyoto, Japan, Model GC Mini2; Photovac Voyager portable gas chromatograph (GC) Perkin-Elmer, Norwalk, Connecticut) was housed in one of the station's air-conditioned laboratories at a clearing where we used it for 10 days of concentration measurements from 5 m above the ground as well as for leaf-level enclosures (J. Herrick et al., manuscript in preparation, 2004). After the initial startup phase, the PTR-MS instrument was transferred to the instrument shed adjacent to the 42 m CARBONO eddy flux tower [cf. *Loescher et al.*, 2004], located ca. 1.8 km into the old-growth forest from the laboratory clearing. In addition to the VOC measurements, NO_x and NO_y concentration gradients (Thermoenvironmental Instruments Inc., 42S, with external converter) were measured at the tower at 5 heights (5–25 m) during the first 2 weeks of the experiment. During the last week of the study, ozone profiles were measured using a UV absorption sensor (Model 202, 2B Technologies, Golden, Colorado). Micrometeorological measurements at the tower were performed using two sonic anemometers; one was mounted at the top (RM Young, 81000, Campbell Scientific, Inc.) for direct eddy covariance measurements and one was installed at various heights inside the canopy (K-Probe, Applied Technologies, Inc.) for obtaining an in-canopy variance profile. The leaf area index was measured indirectly using the LAI2000 (LI-COR, Lincoln, Nebraska). The local leaf area index of 4.23 m^2/m^2 is on the low side of typical landscape-scale level values for this forest (average: 6 m^2/m^2, D. Clark, personal communication) and might therefore not be representative for the whole ecosystem. In the present case we primarily use it as a qualitative measure to illustrate the canopy structure surrounding the tower. Air was pulled through a 50 m teflon line (O.D. = $^1/_4''$) from the top of the sampling tower at a high pumping speed (~15 L/min), reducing the pressure inside the line to 400 mbar in order to avoid water condensation inside the line, minimize memory effects and assure a fast response time. The overall delay time for eddy covariance measurements was 7 s, measured by spiking an isoprene and acetone pulse at the top of the tower. For the gradient measurements two 50 m lines were continuously flushed with the same total flow rate (15 L/min) resulting in delay times of 14 s. The canopy line was pulled by a dolly attached to a computer-controlled winch, and sampled from the ground to 30 m

height. The canopy line was moved at a constant speed of 0.2 m/s resulting in a continuous profile every 3 min. After 2 profiles (every 6 min), we measured the reference concentration at 42 m for 30 s by switching the PTR-MS instrument to the top (42 m) line. The PTR-MS instrument has been described in detail elsewhere [*Lindinger et al.*, 1998]. We have also recently described operational conditions for eddy covariance and disjunct eddy covariance measurements and have characterized response times and damping effects in long lines [*Karl et al.*, 2001, 2002a]. The quantification of VOCs was based on gravimetrically prepared calibration standards with an estimated uncertainty on the order of ±20%. Reference measurements for determining the instrumental background were taken through a catalytic converter (platinum wool at 430°C) and were performed every 30 min to 2 h.

3. Flux Methodology

[6] In general the eddy covariance measurements performed above a forest canopy are related to the source and sink terms according to the mass balance equation,

$$F^{h}_{VOC} + \frac{\partial}{\partial t}\int_{0}^{h} C_{VOC}(z)\cdot dz = -\int_{0}^{h} D_{VOC}(z)\cdot dz, \qquad (1)$$

where F^{h}_{VOC} is the turbulent flux of a VOC at a reference height h, $C_{VOC}(z)$ is the concentration (integrated over height to get the storage term), and $D_{VOC}(z)$ is the height-dependent emission or deposition from surfaces. During daytime the storage term is typically small (<20%) compared to the turbulent flux, whereas at night the contribution of the storage term dominates (>80–90%) and is much larger than the turbulent flux. Daytime disjunct eddy covariance fluxes were calculated following previously published procedures [*Karl et al.*, 2002a; *Rinne et al.*, 2002].

[7] Numerous studies [e.g., *Steffen and Denmead*, 1988] found that transport within canopies cannot be described by a purely diffusive component. Modified K-theory can therefore not be used for calculating source terms based on concentration gradients. Nonhomogeneous diffusion in a dense canopy is typically characterized by a dispersion matrix, which relates the concentration field to individual source/sink layers. We compare three methods for calculating in-canopy diffusion: (1) the localized near field theory (LNF) [*Raupach*, 1986a, 1986b], (2) the continuous near field theory (CNF) [*Warland and Thurtell*, 2000], and (3) a random walk model [*Baldocchi et al.*, 1987]. Input parameters for all methods were based on measured profiles of turbulence (σ_w/u_*) and the estimated Lagrangian Timescale (T_L) [*Raupach*, 1986a],

$$\frac{\sigma_w(z)}{u_*} = \begin{cases} a_1 & z \geq h \\ 0.5\cdot(a_1+a_0) + 0.5\cdot(a_1-a_0)\cdot\cos\{\pi(1-z/h)\} & z < h \end{cases} \qquad (2a)$$

$$T_L(z) = \frac{h}{u_*}\cdot\left\{c_1\left(\frac{z-d}{h}\right) + \left(c_0 + \frac{c_1 d}{h}\right)\cdot\exp\left(\frac{-c_1\cdot z/h}{c_0 + c_1 d/h}\right)\right\} \qquad (2b)$$

with h (canopy height), z (height above ground), $a_1 = 1.1$, $a_0 = 0.1$, u_* (friction velocity), σ_w (standard deviation of the vertical wind velocity), d (displacement height estimated to be ~2/3 of the canopy height), $c_0 = 0.3$, and $c_1 = 0.4/a_1^2$. The parameters a_0 and a_1 were fitted using the measured turbulence profiles (σ_w/u_*). The dispersion matrices (D) were calculated using Lagrangian dispersion theory according to *Nemitz et al.* [2000] and *Warland and Thurtell* [2000] and the random walk model adopted from CANVEG [*Baldocchi et al.*, 1987] as outlined in Appendix A. The source/sink distribution was computed according to

$$\vec{C} - C_{ref} = \overleftrightarrow{D}\cdot\vec{S} \qquad (3)$$

with C (concentration vector), C_{ref} (concentration at reference height), D (dispersion matrix), and S (source/sink vector).

[8] Figure 1 shows a comparison between the outputs of the LNF, the CNF, and the random walk model. The horizontal axis shows the concentration difference from the mean between the three models. On average the calculated deviation between the three methods lies within reasonable uncertainty (±20%), which is encouraging. Based on a given source distribution (following a typical Leaf Area Index (LAI) profile shown on the right panel) the random walk model predicts a higher concentration profile than the CNF approach in the upper part of the canopy. The LNF model typically lies within ±20% of the CNF and random walk model, especially in the upper part of the canopy, where most of the VOC emissions occur. The solution (source S) to the inverse problem (equation (3)) was calculated numerically solving an overdetermined set (concentration layers (z^c) > source layers (z^s)) of equations. In order to achieve satisfying accuracy we found that for each source layer at least two concentration layers should be used. The final source distributions shown in Figures 5 and 6 (middle panels) were calculated using a 20 × 6 dispersion matrix. We do not attempt to separate ground-level emissions from those in the first 2 m due to limitations of the σ_w/u_* parameterization in the "basal layer" [*Wilson and Flesch*, 1993]. A more detailed assessment of the σ_w/u_* parameterization was described by *Nemitz et al.* [2000], who found that despite these limitations close to the ground the net flux above the canopy is not affected. Low wind speeds and stable conditions during nighttime can be problematic. *Siqueira et al.* [2002] compared the CO_2 distribution and net flux of three canopy models with direct eddy covariance measurements at Duke forest, a site characterized by wind speeds that are generally lower than at the present flux tower. In general, nighttime eddy covariance measurements have to be used with caution as they are subject to potential systematic errors at low wind speeds [*Saleska et al.*, 2003]. Assuming that nighttime fluxes can be accurately measured by eddy covariance, *Siqueira et al.* [2002] found that canopy models (including the LNF model) in general overpredict the net CO_2 flux during nighttime. A regression between the net CO_2 flux inferred from the LNF model and measured by eddy covariance yielded a slope of 0.74 for unstable and stable and 1.3 for neutral conditions. The maximum difference between eddy covariance and the ILT model during nighttime was reported to be a factor of 2. During nighttime our

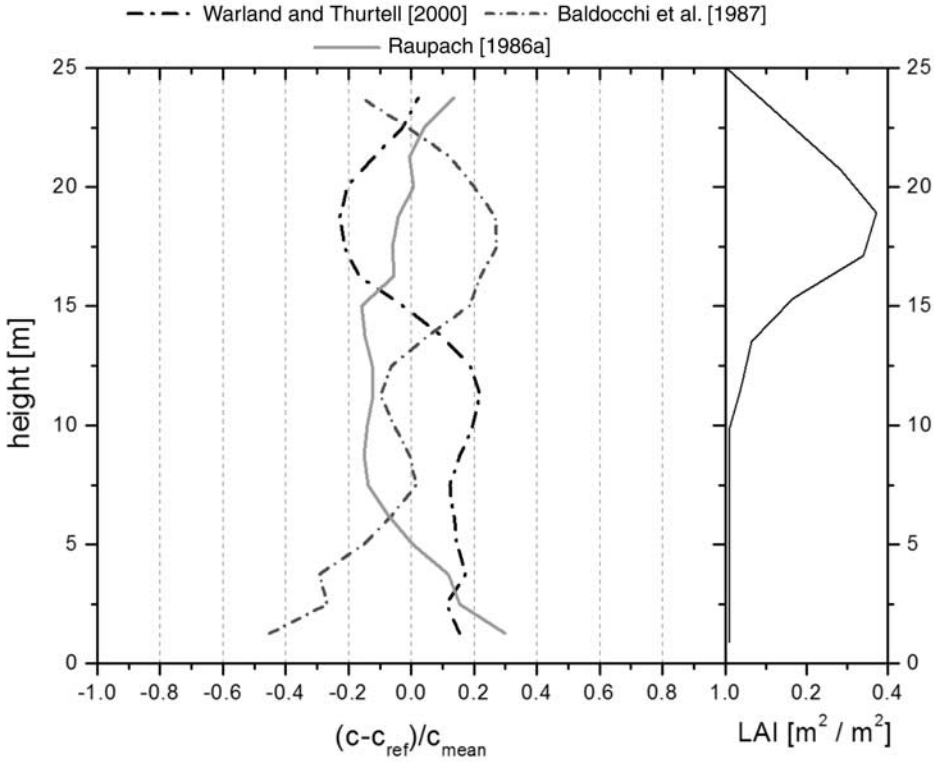

Figure 1. Comparison of the calculated concentrations between the LNF [*Raupach*, 1986a], the CNF [*Warland and Thurtell*, 2000], and the random walk [*Baldocchi et al.*, 1987] models, based on a given source profile following the LAI profile shown on the right side and expressed as a relative deviation from the mean. See color version of this figure at back of this issue.

measurements suggest that part of the deviation between the gradient and eddy covariance method occurs due to formation of an inversion layer at the top of the canopy [*Fitzjarrald and Moore*, 1990], which decouples air masses above and below the forest canopy. If the reference height of the concentration measurement lies above the inversion layer, the net flux based on canopy gradient models is systematically overpredicted.

4. Results

4.1. Observed VOCs at La Selva

[9] The selectivity of the PTR-MS technique has recently been investigated thoroughly in a variety of field deployments [*de Gouw et al.*, 2003a, 2003b; *Warneke et al.*, 2003; *Kuster et al.*, 2004]. In the present study the major VOCs detected by the PTR-MS technique were methanol (m/z 33+), acetonitrile (m/z 42+), acetaldehyde (m/z 45+), acetone (m/z 59+), formic acid (m/z 47+), acetic acid (m/z 61+), isoprene (m/z 69+), the sum of all $C_{10}H_{16}$ monoterpenes (m/z 81+ and m/z 137+), MVK+MACR (m/z 71+), benzene (m/z 79+), and toluene (m/z 93+). The collisional energy in the drift tube of the PTR-MS instrument was high enough to fragment a significant fraction (>90%) of ethanol (m/z 47+) into m/z 19+ and reduce interference with formic acid detection. Other interferences at m/z 61+, such as photochemically produced glycolaldehyde, were assessed using the NCAR Master Mechanism (MM) [*Madronich and Calvert*, 1989] and appeared to be minor (<10%). We consistently observed a diurnal cycle on m/z 47+, paralleling that on m/z 61+. The mean concentrations observed on m/z 61+ (1 ppbv) and m/z 47+ (1.3 ppbv) at La Selva are comparable to measurements of gas-phase formic and acetic acid performed in a tropical cloud forest in Costa Rica [*Sanhueza et al.*, 1992], who report 1.7 and 1.4 ppbv for HCOOH and CH_3COOH, respectively, during the dry season. We therefore mainly attribute formic and acetic acid to m/z 47+ and m/z 61+, respectively. This assumption is supported by recent field observations of acetic acid by *de Gouw et al.* [2003b], who compared ambient measurements of the PTR-MS instrument with those obtained from a fog chamber.

[10] Typical diurnal cycles measured at 5 m above the ground in the main laboratory clearing (average: dashed dotted lines) and at the top of the 42-m-tall tower in old-growth forest (ca. 1.8 km SW of the laboratory clearing) (average: solid lines) are shown in Figures 2a and 2b. In general, the concentration patterns at both locations are similar, suggesting a rather homogenous distribution of these compounds, as expected for species that are primarily derived from biogenic sources (e.g., isoprene and monoterpenes) and from atmospheric oxidation of precursor compounds (e.g., MVK+MACR). Ambient concentrations of the isoprene oxidation products MVK+MAC are comparable to mixing ratios found in the Amazon [*Kesselmeier et al.*, 2002a].

[11] Tracer compounds for biomass burning (acetonitrile: m/z 42+) and primary anthropogenic emissions (benzene m/z 79+, toluene m/z 93+) were used to assess disturbances (Figure 2b) and reached similar concentrations at the tower

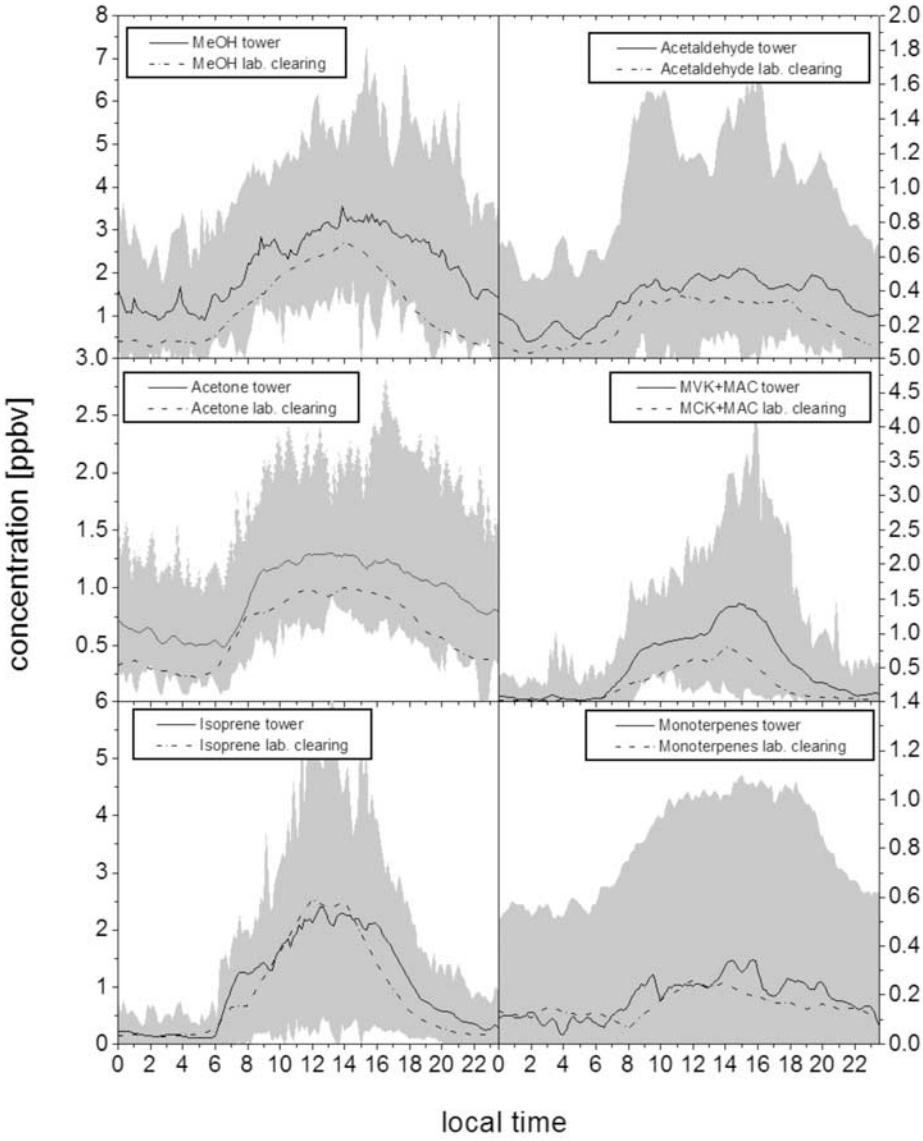

Figure 2a. Ambient concentrations measured at the laboratory clearing (dashed line) and tower (solid line). The gray shaded area represents the concentration range observed during the whole study at the tower.

and the laboratory clearing (for clarity, only the data from the laboratory clearing are shown). Benzene and toluene concentrations were in general low during daytime (ca. 15 pptv) and increased during nighttime up to 100 pptv. This is consistent with the idea of evenly distributed anthropogenic background emissions building up during nighttime due to the collapse of the boundary layer. Mean acetonitrile mixing ratios showed a pronounced diurnal cycle with mean daytime concentrations (300 pptv) higher than nighttime concentrations (100 pptv) and the lowest concentrations (80 pptv) typically occurring in the early morning. We attribute this cycle to an increased diurnal background building up during daytime due to small-scale biomass burning activities and a decrease after sunset driven by dry deposition. Even though the study was conducted at the end of the dry season, distant burning activities, e.g., on plantations, were observed from the tower on several occasions. The opposite diurnal cycles of acetonitrile, benzene, and toluene suggest that the later two compounds are not produced by biomass burning to a great extent, but are related to diffuse area sources such as cars and diesel generators, found both at the La Selva station and in the surrounding region, and commonly used throughout the rural tropics. It also argues that acetonitrile emissions are greater and benzene and toluene emissions are smaller than dilution effects caused by the growing boundary layer during daytime.

[12] The average time since emission of isoprene (t) and its detection at the inlet was determined from the ratio of isoprene and its oxidation products MVK+MAC, as depicted in Figure 3. During daytime the average ratio MVK+MAC to isoprene was 0.54, well within the range (0.1–1.7) observed in other tropical ecosystems [*Andreae et al.*, 2002; *Kesselmeier et al.*, 2002a]. We can define an average relative age since emission (t/τ) with respect to the

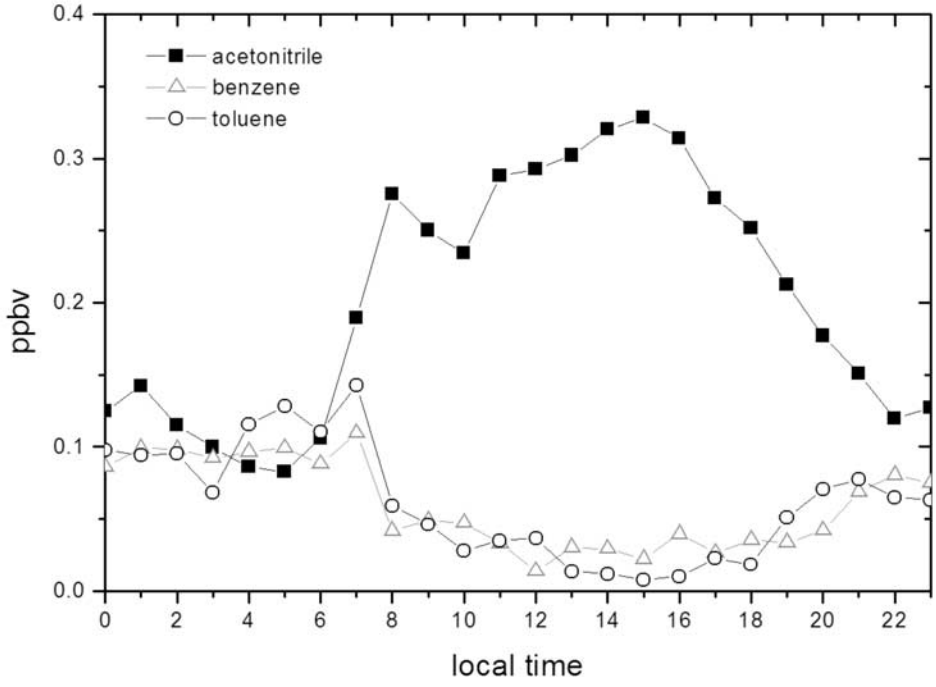

Figure 2b. Average diurnal concentration cycle of benzene, toluene, and acetonitrile at the laboratory clearing.

photochemical lifetime (τ) for the mean concentration measurement of isoprene. This ratio followed a Gaussian distribution centered on 0.5 at the laboratory clearing and 0.8 at the tower. Thus, assuming an average photochemical lifetime of 40 min during the day, the average age of the mean isoprene abundance would be 20 and 32 min at the laboratory clearing and tower, respectively; the footprint of the isoprene concentration measurement can subsequently be estimated to be within 2.4 and 3.8 km at an average wind speed of 2 m/s. The footprint for the flux measurement

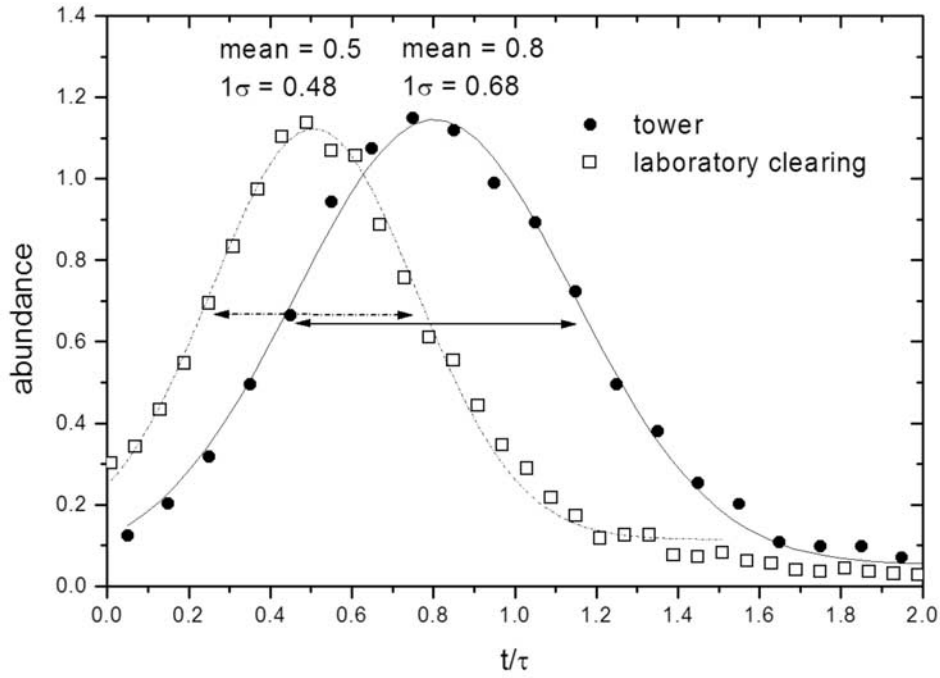

Figure 3. Distribution of the ratio between isoprene and its oxidation products MVK+MAC expressed as ratio between time since emission (t) and photochemical age (τ).

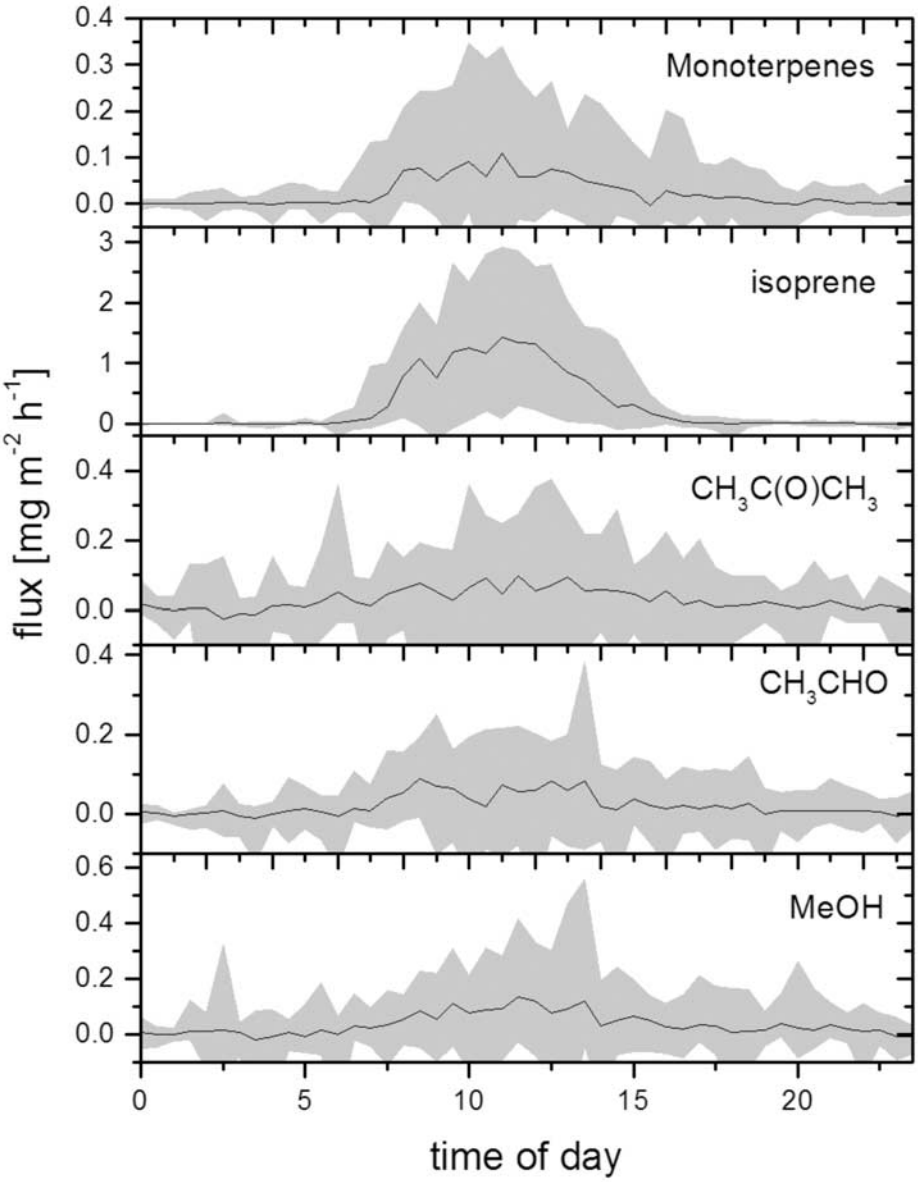

Figure 4. Diurnal cycle of fluxes observed by eddy covariance. The gray area depicts the range observed at the site during 3 weeks of measurements.

under unstable conditions was estimated to be even smaller (<1 km) according to *Horst and Weil* [1992].

4.2. Fluxes Measured by Disjunct Eddy Covariance

[13] Figure 4 depicts diurnal fluxes measured by disjunct eddy covariance at the top of the 42 m tower between April 16 and May 5, 2003. During 4 days within this period, gradient measurements were performed. General aspects of disjunct sampling strategies have been described in detail elsewhere [*Rinne et al.*, 2001; *Karl et al.*, 2002a]. Mean (maximum) midday net fluxes were on the order of 0.13 (0.5), 0.08 (0.2), 0.09 (0.36), 1.35 (2.9), and 0.1 (0.33) mg m^{-2} h^{-1} for methanol, acetaldehyde, acetone, isoprene, and the sum of monoterpenes, respectively. The isoprene flux (1–3 mg mg m^{-2} h^{-1}) is comparable to previous canopy scale measurements (2.5 mg m^{-2} h^{-1}) at the same tower during the high-rain month of October 1999 using the relaxed eddy accumulation method [*Geron et al.*, 2002] and followed the expected light and temperature dependence. A more detailed assessment of leaf level and canopy scale isoprene emissions will be presented elsewhere (J. Herrick et al., manuscript in preparation, 2004).

[14] In contrast to leaf level measurements by *Geron et al.* [2002], who screened 20 common tree and liana species from this forest, the present study shows a significant release of monoterpenes with a total flux up to 0.33 mg m^{-2} h^{-1}. Furthermore our observations of maximum fluxes (and concentrations) during daytime show that total monoterpene emissions are light- and temperature-dependent (Table 1). *Kuhn et al.* [2002a], for example, found that the tropical species *Apeiba tibourbou* mainly emitted sabinene, a-pinene, and b-pinene in a very similar light- and temperature-

Table 1. Temperature- and Light-Dependent Emission Parameters as Well as the Linear Regression Parameters ($F_{VOC} = A_{wT} \times wT + B_{wT}$) With Respect to Sensible Heat Fluxes, the Estimated Total Emission as a Fraction of the NEE of CO_2-C Estimated for the La Selva Forest in 1999 by Eddy Covariance [*Loescher et al.*, 2003], and Extrapolated Yearly Emissions for Tropical Forests

	β, K^{-1}	E_0, g m^{-2} h^{-1}	A_{wT}, g W^{-1} h^{-1}	B_{wT}, g m^{-2} h^{-1}	Error	R	Percent NEE	Source, Tg yr^{-1}
MeOH	0.13	2.0E-04	9.94E-07	1.08E-04	±20%	0.67	0.11–0.75	8–62
Acetaldehyde	0.19	1.4E-04	7.45E-07	7.62E-05	±30%	0.66	0.11–0.44	6–24
Acetone	0.20	2.1E-04	1.14E-06	1.04E-04	±30%	0.73	0.16–0.61	8–29
	α[a] [PAR^{-1}]	$Cl \times E_0$[a]						
Isoprene[b]	0.00073	0.00172	7.98E-06	9.90E-05	±10%	0.87	2.5–3.5	90–124
Monoterpenes[c]	0.00097	0.00013	7.32E-07	1.06E-04	±20%	0.65	0.19–0.23	6–8
Total							3.1–5.5	120–250

[a]The light and temperature dependence was modeled according to $E(PAR, T) = \frac{\alpha \cdot Cl \cdot E_0 \cdot PAR}{\sqrt{1+\alpha^2 \cdot PAR^2}} \cdot \frac{C_{T2} \cdot e^{C_{T1} \cdot x}}{C_{T2} - C_{T1} \cdot e^{C_{T2} \cdot x}}$, with $x = \left(\frac{1}{T_{opt}} - \frac{1}{T}\right)/0.00831$.

[b]Temperature dependence from *Geron et al.* [2002] and J. Herrick et al. (manuscript in preparation, 2004).

[c]Temperature dependence taken from the whole canopy parameterization used by *Guenther et al.* [1995] and *Guenther* [1997].

dependent fashion. Our canopy level observations confirm and generalize previous leaf level measurements of various tropical species. The total monoterpene flux inferred from our eddy covariance measurements (Figure 4) is also comparable to the sum of alpha and beta pinene fluxes observed above the Amazon by *Rinne et al.* [2002]. In addition, our in-canopy profiles suggest that at least part of the nighttime abundance was likely related to herbivory. A more detailed assessment of VOC emissions due to wounding will be presented elsewhere (J. Sparks et al., manuscript in preparation, 2004).

[15] Acetone fluxes obtained from the current study (maximum: 0.36 mg m^{-2} h^{-1}) are substantially lower than those reported by *Geron et al.* [2002], who found emissions up to 2.2 mg m^{-2} h^{-1}. Similarly we observed methanol fluxes that were a factor of 3 lower compared to those measured by *Geron et al.* [2002], but additional eddy flux measurements are required to determine if these differences are due to seasonal variations or because of the small number of wet season samples and the relatively large uncertainties associated with the cartridge REA measurements. Seasonal variations in net fluxes of acetone and methanol could be due to changes in ecosystem function or a result of increased deposition from regional biomass burning during the dry season. Our measurements (both DEC and the ILT method) suggest that acetone is predominantly emitted during daytime, in contrast with observations by *Andreae et al.* [2002], who report deposition fluxes of acetone of 232 ng m^{-2} s^{-1} during the day. Assuming no biogenic acetone emissions and taking typical acetone concentrations observed in the tropics between 0.8 to 3 ppbv [*Kesselmeier et al.*, 2002b; *Poeschl et al.*, 2001, this work], these values would correspond to deposition velocities on the order of 3–12 cm/s and would be as fast as those of nitric acid. Even though the total canopy flux of acetaldehyde is comparable to acetone, the gradient measurements (see next section) show quite different emission patterns between these two carbonyl compounds.

[16] Table 1 summarizes the observations of VOC fluxes obtained from the present study. Fluxes of oxygenated compounds are mainly temperature-driven and follow an exponential dependence of the form of $E_0 \times \exp(\beta \times (T - T_s))$, where E_0 is the flux at standard conditions (e.g., g m^{-2} h^{-1}), T is temperature (K), T_s is the standard temperature (here 303 K), and β is a fitting parameter (K^{-1}). Isoprene and monoterpene emissions show both light and temperature dependence (J. Herrick et al., manuscript in preparation, 2004). Fitting of the light-dependent parameters α and Cl using the current data set was compared to the whole canopy parameters inferred from the Sun and shade leaf model from *Guenther et al.* [1995]. The parameters agreed within ±30% and are listed in Table 1. The temperature range for conditions above 1000 PAR was too small (28–32°C) in order to reliably fit the temperature-dependent parameters (C_{t1}, C_{t2}, T_{opt}) for isoprene and monoterpene emissions according to the G97 algorithm [*Guenther*, 1997]. However, we found that standard values for the individual parameters C_{t1}, C_{t2}, and T_{opt} [*Guenther*, 1997] could reproduce isoprene and monoterpene fluxes observed at this site. For all compounds a reasonable linear correlation with sensible heat fluxes wT was found [cf. *Rinne et al.*, 2001; *Westberg et al.*, 2001; *Karl et al.*, 2002b]. These relationships could potentially be used instead of traditional temperature and light parameterizations. Taking upper and lower limits of the temperature- and light-dependent parameterizations based on our measurements together with environmental data from the year 1999 [*Loescher et al.*, 2003], we estimate that potentially up to 86 kg C/ha/yr, or 5.5% of NEE, can be lost in form of methanol, acetaldehyde, acetone, isoprene, and monoterpenes. This is somewhat lower than previous estimates [*Geron et al.*, 2002; *Kuhn et al.*, 2002a; *Kesselmeier et al.*, 2002b] but 3 orders of magnitude higher than the estimated carbon source of carbonaceous aerosols [*Loescher et al.*, 2004]. The last column in Table 1 depicts the extrapolated range of yearly emissions from tropical forests assuming similar conditions and a total area of 19.8×10^6 km^2 [*Guenther et al.*, 1995].

[17] The best estimate of the total extrapolated emission of methanol, acetaldehyde, and acetone, respectively, are 6.7, 4.4, and 6.1 kg C/ha/yr, or 0.43%, 0.28%, and 0.39% of net ecosystem exchange (NEE) for this tropical forest. The production of methanol is linked to plant growth [*Fall*, 2003], and there have been attempts for upscaling methanol emissions based on net primary production (NPP) [*Galbally and Kirstine*, 2002]. Unfortunately estimates of NPP for tropical forests have been based on incomplete and often problematic field measurements [see *Clark et al.*, 2001]. *Curtis et al.* [2002] recently investigated the carbon exchange at five deciduous North American forests based on a detailed biometric study. They estimated that on average NPP was 2.9 ± 0.42 times higher than NEE. *Malhi et al.* [1999] found a similar ratio (2.6) for a tropical rain forest in the Amazon. In order to compare our results for methanol with assumptions made for a global methanol

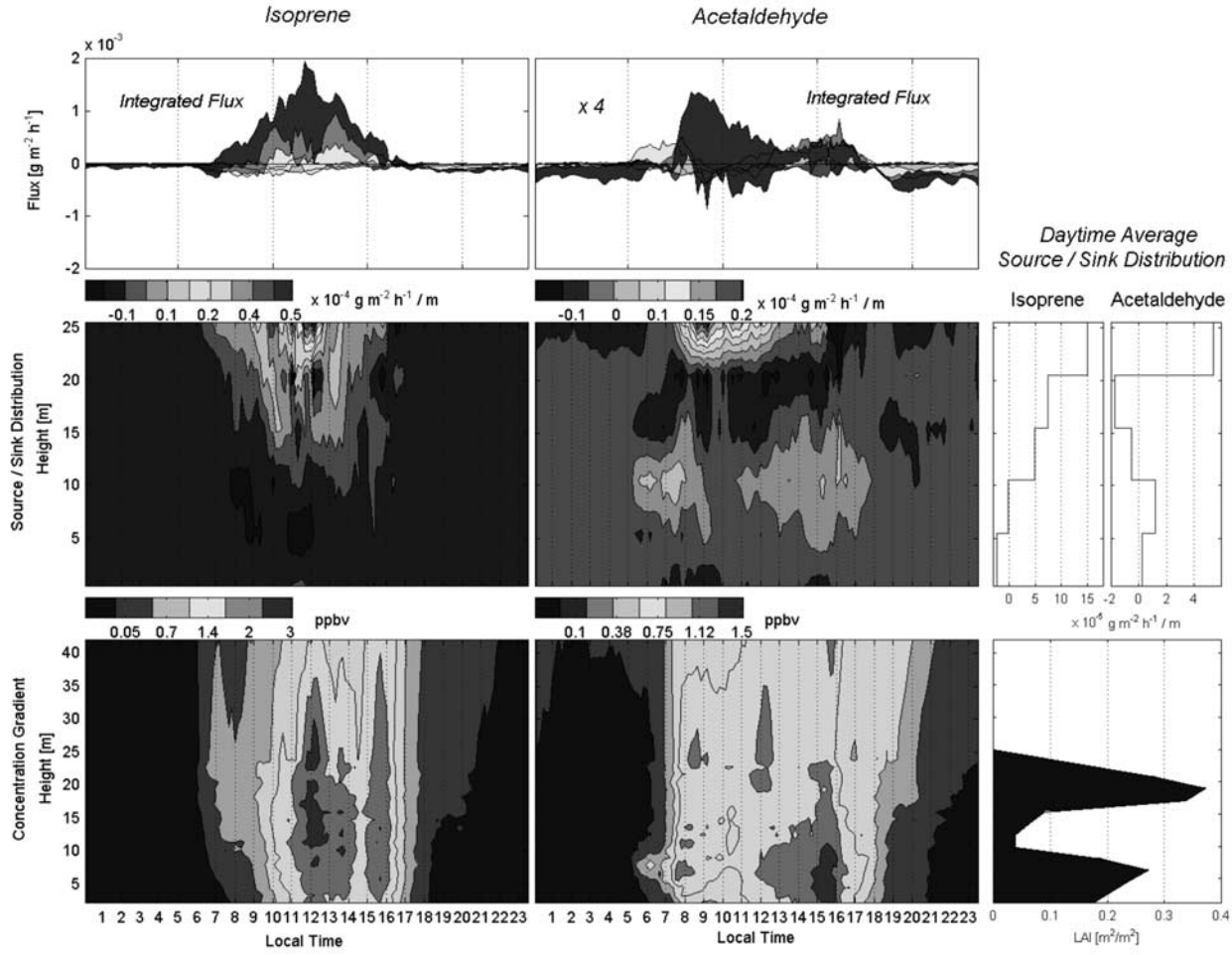

Figure 5. (bottom left and center) Averaged contour plots of isoprene and acetaldehyde concentrations as a function of local time (*x* axis) and height above ground (*y* axis). (bottom right) Measured leaf area index (LAI). (middle left and center) Calculated source/sink distribution of isoprene and acetaldehyde as a function of local time (*x* axis) and height above ground (*y* axis). (middle right) Averaged source/sink distribution during the day. (top) Total fluxes integrated over individual source/sink layers; the color-coding indicates the relative difference between subsequent source/sink layers, and the dark red color represents the top layer. See color version of this figure at back of this issue.

budget [*Galbally and Kirstine*, 2002] we take the above ratio (NPP:NEE) of 2.6 ± 0.42. The emission factor related to productivity for methanol would then roughly equal $(0.17 \pm 0.06)\%$ of NPP. This is ~50% higher than the generic value of 0.11% applied in the global methanol assessment presented by *Galbally and Kirstine* [2002]. Our emission factors for acetaldehyde and acetone, with a normalized average emission at 30°C of 0.14 and 0.21 mg m^{-2} h^{-1}, respectively, are somewhat smaller than those previously reported at La Selva [*Geron et al.*, 2002] and at a deciduous forest in northern Michigan [*Karl et al.*, 2003].

4.3. Gradient Measurement

[18] The fine-scale source distribution of VOCs was obtained by a canopy profiling system as described in the experimental section. The profiles were run for 2 consecutive days in the second and third week of measurements at the tower. The obtained data set was averaged over 1 hour and binned in 1 m vertical slices. In order to compare with the eddy covariance measurements, the individual profiles were averaged for the 4 days, which were all characterized by similar weather conditions (no rain event in the late afternoon nor during the night). The advantage of having a moveable inlet is twofold: (1) memory effects or contamination due to multiple lines can be excluded, and (2) the data can be averaged/binned in an optimal way during postprocessing. As outlined by *Nemitz et al.* [2000], the number of input heights can be important for exchange processes that occur in a shallow height range. The continuous gradient measurement makes sure that these processes are resolved and not lost due to a limited set of measurements. As an example, the bottom panels in Figure 5 (Figure 6) show a composite of the vertical distributions of isoprene (methanol) on the left and acetaldehyde (acetone) on the right side. The measured leaf area index (LAI) is plotted as a function of height on the very right bottom panel and is characterized by a bimodal distribution, which is frequently observed in the tropics [*Golley and Hartshorn*, 1984]. Isoprene (Figure 5) has its maximum concentration (~3 ppbv) in the upper part of the canopy (~15–30 m)

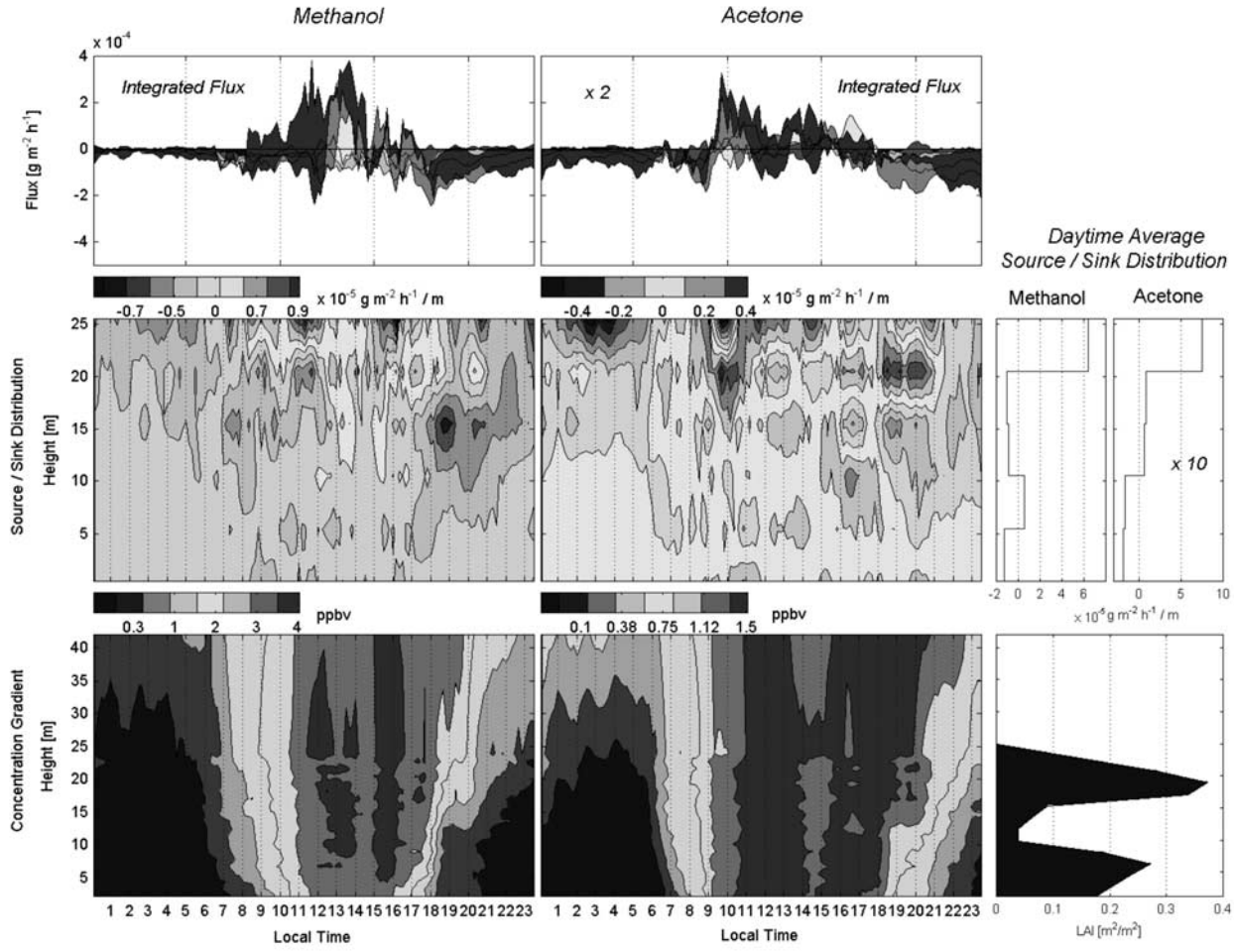

Figure 6. Same as Figure 5 for methanol and acetone. See color version of this figure at back of this issue.

during midday, falling off toward the ground and above 30 m. This is consistent with the fact that light-dependent isoprene emissions occur in the upper part of the canopy. Isoprene emissions start to decrease in the early afternoon (1400–1500 LT). The concentration increase around 1530 LT is most likely due to decreased turbulence and a collapsing boundary layer, which also causes enhanced acetaldehyde, acetone, and methanol concentrations. The lower middle panel in Figure 5 illustrates that acetaldehyde mixing ratios (~1–1.5 ppbv) accumulate in the lower part of the canopy (~0–10 m) during daytime. This pattern suggests that this compound has a substantial source in the understory. While methanol concentrations (Figure 6, left panel) are clearly enhanced (up to 4 ppbv) below 23 m (top of canopy), the acetone canopy gradient (Figure 6, bottom middle panel) is somewhat less pronounced with mixing ratios up to 1.5 ppbv during daytime. In both cases we observe a strong nighttime gradient discussed in the next section.

4.4. Inverse Lagrangian Transport Model: Source/Sink Distribution

[19] The source/sink distributions as a function of height (y axis) and time of day (x axis) for isoprene, acetaldehyde, methanol, and acetone are plotted in Figures 5 and 6 (middle panels). The highest emissions of isoprene (Figure 5, left middle panel) occur at noon in the uppermost part of the canopy with a source strength up to 4×10^{-4} g m^{-2} h^{-1}/m, while it can be lost (deposited) below 10 m at a rate of -0.5×10^{-4} g m^{-2} h^{-1}/m. In general, our analysis does not explicitly account for photochemical losses/production, which is therefore convoluted with direct sources and sinks. The average daytime source/sink distribution is plotted on the right side binned according to 6 source/sink layers. The layer up to 5 m consistently acts as a sink during daytime. The source strength between 5 and 10 m is close to zero and positive above 10 m. From this plot it can be calculated that the loss region comprises about ~10% of the total source strength. A mean below-canopy daytime HO density of 5×10^4 molecules/cm^3 would be sufficiently high to cause the observed isoprene loss in the lower part of the canopy. Independently we can estimate the overall photochemical loss from the ratio of MVK+MAC to isoprene considering turbulent exchange times of ~100 s during daytime (based on the far field limit of Lagrangian dispersion). From this analysis it can be estimated that less than 10% of isoprene is oxidized within the canopy.

[20] Thus, even though reaction with HO radicals in the lower part of the canopy can oxidize part of the emitted isoprene, the bias for the overall isoprene flux measurement

is relatively small. The contour plot on the right depicts acetaldehyde, which shows a completely different emission/deposition pattern. A source region between 5 and 15 m, corresponding to the understory (lower peak of LAI), is followed by a net sink layer in the lower part of the crown region and a production layer in the uppermost part of the canopy. Acetaldehyde emissions in the midcanopy (5–15 m) contrast recent measurements by *Cojocariu et al.* [2004], who observed steadily declining acetaldehyde emissions from the top to the bottom of a spruce canopy. We attribute the increased acetaldehyde emissions in the lower part of this tropical forest to (1) a change in biomass density and (2) the possibility of a different production mechanism related to light flecks. In previous laboratory studies [*Holzinger et al.*, 2000; *Karl et al.*, 2002b], acetaldehyde spikes were consistently observed following light-dark transitions. These acetaldehyde bursts were explained by the accumulation of cytosolic pyruvate, triggering the pyruvate decarboxylase reaction [*Karl et al.*, 2002b] and were not related to the oxidation of ethanol, which can also trigger the formation of acetaldehyde in leaves [*Kreuzwieser et al.*, 2000]. We hypothesize that acetaldehyde emissions from this ecosystem could be due to a combination of conversion of cytosolic pyruvate and the oxidation of ethanol. The panel on the very right averages the emission/deposition profile for acetaldehyde during daytime hours. The source strength in the lower part accounts for up to 27% of the total acetaldehyde emission. The forest also recaptures part of the emission; the total canopy sink comprises about 43% of the total source strength. The highest emissions occur at the top of the canopy. The mean acetaldehyde production rate obtained from the middle panel in Figure 5 is 1.3×10^{-4} g m^{-2} h^{-1}/m. Can this rate be explained by the photooxidation of precursor compounds (e.g., ethane, propane, propene)?

[21] Taking an upper limit of 2.5×10^6 molecules/cm^3 [*Jacob and Wofsy*, 1988] for the average HO density (between 0800 and 1400 LT) in the surface layer the concentration of precursor compounds would need to be as high as 425 ppbv for ethane, >43 ppbv for other alkanes and >3.4 ppbv for propene in order to explain the observed acetaldehyde production rate. These mixing ratios would be at least 1 order of magnitude higher than typical values observed in the tropics [e.g., *Greenberg and Zimmerman*, 1984]. From the PTRMS data set we estimate an upper limit of propene (m/z 43+) concentrations after correcting for the abundance of acetic acid (~26%) and acetone (~5%) on m/z 43+. The residual median concentration between 0700 and 1500 LT yielded 0.71 ± 0.22 ppbv. This most likely also includes other compounds (e.g., propanol) as $C_3H_7^+$ is a common fragment. We therefore conclude that acetaldehyde emissions at the top are primarily of biogenic origin. Even though the overall net flux of acetaldehyde and acetone during daytime are very similar, the individual source/sink layers obtained from the gradient measurements within the canopy are quite different. Figure 6 depicts methanol and acetone, which show a similar exchange pattern. The emission occurs mainly during daytime in the upper part of the canopy. After sunset, we observe a significant sink below the crown region, just above the minimum LAI in the middle of the canopy. The top panels in Figures 5 and 6 depict the integrated source/sink layers and correspond to the net exchange at the canopy top. The calculated flux at the top should therefore be comparable to the flux measured by the eddy covariance method.

4.5. Comparison Between Disjunct Eddy Covariance and Lagrangian Dispersion

[22] Figure 7b compares the isoprene flux obtained by the ILT model (blue line) with the mean flux (black) measured by disjunct eddy covariance. In general, we observe good agreement between both methods during daytime. After sunset, the ILT model seems to show higher deposition fluxes than the eddy covariance measurements at the 42 m level (pink line). For methanol (Figure 7a) as well as other compounds such as acetone, acetaldehyde, and MVK+MAC (not shown) we get a similar behavior: the net exchange during daytime in general agrees between the eddy covariance and the ILT model; during nighttime there is a systematic offset. By varying the reference height z_{ref} used for the ILT model it appears that ambient concentrations at the 42 m level are systematically enhanced after sunset. We attribute this to the development of an inversion layer, which decouples air masses above from below the crown region. Strong nocturnal radiative cooling at canopy top effectively inhibits most of the exchange between the canopy below the crown and the atmosphere. This phenomenon is frequently observed in tropical ecosystems [*Fitzjarrald and Moore*, 1990] and confirmed by a slightly negative sensible heat flux (wT) shown in Figure 7c. In the late afternoon as the sensible heat flux typically becomes negative over this primary rain forest, a sharp stable potential temperature gradient isolates the canopy from the atmosphere for long periods of time. By readjusting the reference height below the crown region (z_{ref} = 22 m; middle of the upper canopy) during night, we get better agreement (blue line) between the net exchange measured by the ILT model and eddy covariance method. The pink line (Figure 7) shows the case for z_{ref} = 42 m. The eddy covariance flux measurements were always performed at the 42 m level and therefore in general do not adequately capture loss processes occurring below inversion layer of the forest. In addition the deposition flux was in general close or below the flux detection limit of the eddy covariance method. Evidence for loss processes below the crown region was independently inferred from the storage term in the canopy, shown in Figure 8. All compounds exhibit an exponential decay throughout the night, that agrees within a factor of 2 compared to the deposition calculated by the ILT model at z_{ref} = 22 m. In the past, nighttime growth of CO_2 within the canopy, for example, was a standard way to estimate the respiration rate of the forest ecosystem [*Woodwell and Dykeman*, 1966]. The substantial uptake of VOCs by the forest during nighttime is at least part of the reason that ambient concentrations in the surface layer just above the canopy typically show a minimum in the early morning during the breakdown of the inversion, while depleted in-canopy air masses efficiently dilute the surface layer air above. The observed diurnal cycle of VOC concentrations above this tropical forest is therefore related to (1) venting of VOC depleted canopy air and (2) growing of the boundary layer. Figure 9 summarizes the mean daytime (solid line) and nighttime (dashed line) emission and

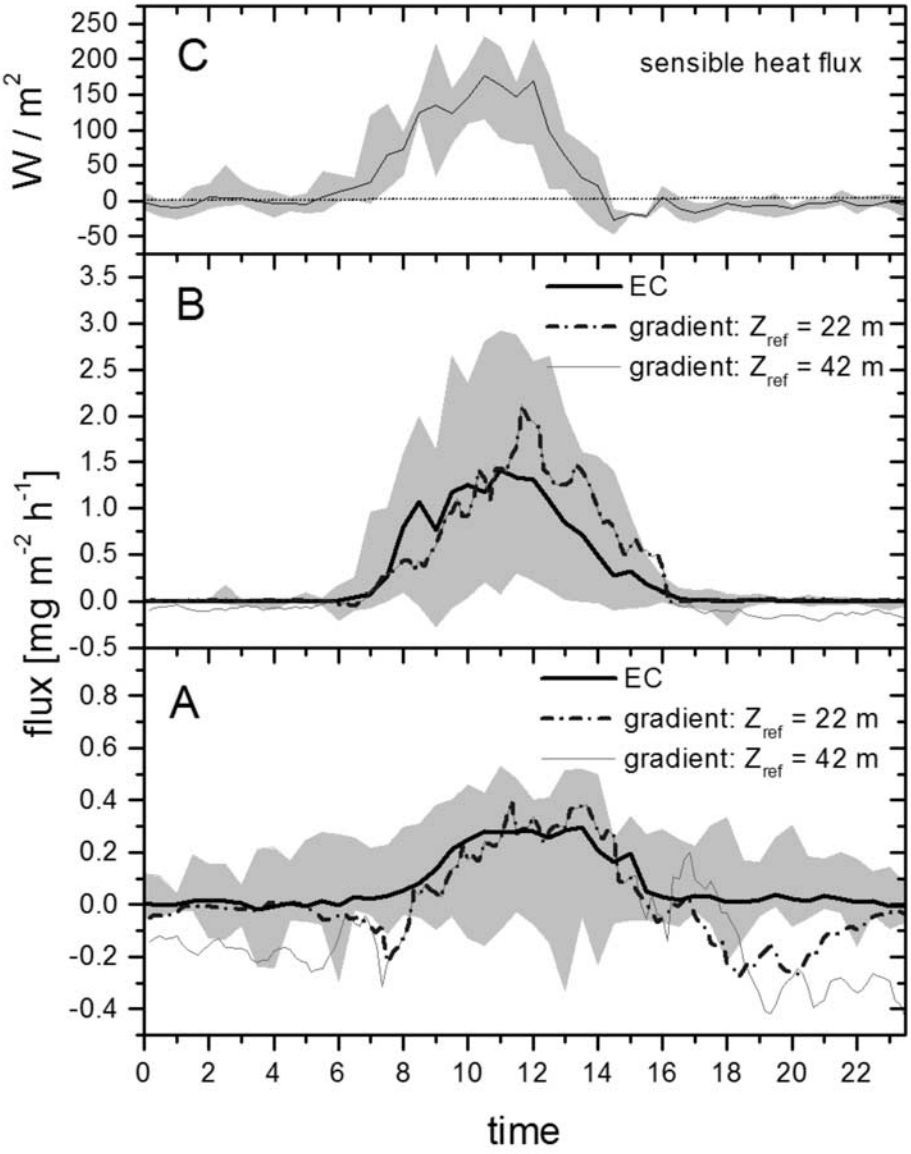

Figure 7. (a) Comparison between the flux obtained by disjunct eddy covariance (black) and the ILT model (blue) for methanol. The pink line illustrates the offset of the ILT model due to a reference height (42 m) above the inversion layer during night; (b) same plot for isoprene; (c) average diurnal cycle of the sensible heat flux during the whole study (dashed line marks zero). The gray area illustrates the range of fluxes observed during the whole campaign. See color version of this figure at back of this issue.

deposition measured for methanol, acetaldehyde, acetone, isoprene, and MVK+MAC based on a reference height of 22 m between 1800 and 0600 LT. Individual loss/production layers within the canopy are represented by a local flux rate (v_d), which was defined as the source strength (s_a) divided by the local concentration (c_a) and has the same dimensions as a deposition velocity. A positive local flux rate indicates local production and a negative value local destruction. Again, it is noted that potential photochemical production or loss (e.g., for MVK+MAC) is included in this term. From Figure 9 it appears that the overall deposition of MVK+MAC was smaller during daytime due to an effective production/source layer above z/h > 0.7, most likely due to the oxidation of isoprene. During nighttime most of the loss of oxygenated compounds occurs in the middle of the canopy (z/h = 0.5). Most of the daytime emission occurs at the canopy top. Isoprene shows a sink in the lower 20% (z/h < 0.2) of the canopy. *Cleveland and Yavitt* [1997] estimated a potential sink for isoprene expressed as a deposition velocity of 0.01 cm/s for tropical soils. This is substantially lower than the average total (dry deposition plus oxidation) daytime sink, equivalent to a deposition rate of 0.16 cm/s, for z/h < 0.2 observed in the present study. As outlined earlier, oxidation via HO radicals could explain this isoprene loss. However, the overall magnitude of the sink below z/h = 0.2 is small (10%) compared to the isoprene emission occurring at the top of the canopy.

[23] During nighttime, oxidation via O_3 and NO_3 can play a role for isoprene and monoterpenes, but not for

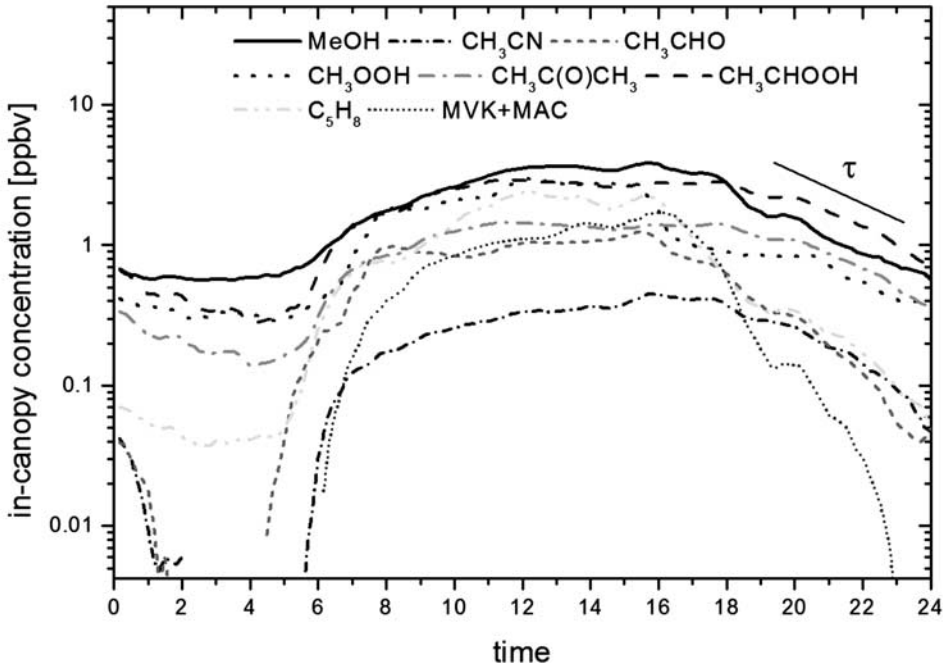

Figure 8. Average diurnal cycle of VOCs within the canopy obtained from the gradient measurements on 4 days during the study. See color version of this figure at back of this issue.

oxygenated VOCs such as methanol and acetone. Owing to ongoing production attributed to a combination of wounding (J. Sparks et al., manuscript in preparation, 2004) and temperature-dependent emissions during night, we were not able to determine deposition rates for monoterpenes. Most oxygenated VOCs show common loss characteristics during nighttime. The mean deposition velocities obtained for formic and acetic acid (0.15 cm/s) are in the range (0.17–0.23 cm/s) of values reported by *Kuhn et al.* [2002b] above a tropical forest in Amazonia. Since stomata are closed during night, it appears that our observed dry deposition rates result in a low residual canopy resistance (R_c). Table 2 examines potential loss mechanisms and compares our observations with traditional deposition routines including the formation of dew. It is obvious for most cases that the measured loss is significantly larger than predicted by traditional deposition models [e.g., *Wesely*, 1989]. The range and uncertainty of the measured deposition velocities in column 5 reflect differences between the ILT model and individual decay rates inferred from the storage term analysis. The effect of nighttime chemistry was assessed using a zero-dimensional box model (NCAR Master Mechanism) [*Madronich and Calvert*, 1989]. The model was initialized as a nondiluting box constrained by the measured mean diurnal cycles of VOC, ozone, and NO_x concentrations and simulated daytime j-values for clear skies. Though the absolute NO_x concentration was held fixed, the relative concentrations of NO and NO_2 were allowed to vary in the model over the course of a day. The last day of a 5-day simulation period was used to assess potential losses due to chemical degradation. NO_3 radicals were calculated to reach concentrations up to 4 pptv with 1–2 ppbv of NO_x available. If these concentrations are sustained within the canopy, NO_3 chemistry could explain the loss of isoprene. For other compounds, nighttime chemistry seems to play a minor role.

[24] Up to 50% of the vegetation [*Pierson et al.*, 1986] is typically covered by dew in the morning. Can the formation of dew in principle explain the observed deposition rates?

[25] To answer this question, we perform a simple "back on the envelope" calculation: Assuming conditions close to equilibrium and a dewdrop concentration ranging between 1.9 and 4.8 g/cm^2 [*Chameides*, 1987] at the end of the night, the total liquid volume present in the 23 m column is on the order of 19–68 L (taking a LAI of 4.22–6 m^2/m^2 and canopy height h of 23 m). For comparison, *Sanhueza et al.* [1992] measured water deposition rates between 31 and 114 mL m^{-2} h^{-1}. Assuming a 12-hour accumulation time, a LAI of 6 m^2/m^2, and canopy height of 23 m, these formation rates are comparable and can potentially add up to 37–162 l for a tropical cloud forest. The maximum decrease of the ambient concentration c_a due to liquid uptake can be estimated according to

$$c_a = \frac{k_v \cdot m_0}{V_l - k_v \cdot V_g}, \qquad k_v = \frac{100}{H \cdot R \cdot T} \tag{4}$$

with c_a (ambient concentration), m_0 (total mass of VOC in the column), V_l (liquid volume), V_g (gas phase volume), k_v (dimensionless partition coefficient), and H (Henry's law constant in M/atm). For a liquid volume of 38 L and Henry's law constants H ranging between 15 (acetaldehyde) and 220 (methanol) M/atm, the ambient concentration in the canopy air can theoretically be reduced by 34–90%. Uptake by dew for a 23 m canopy (h) and duration T was calculated

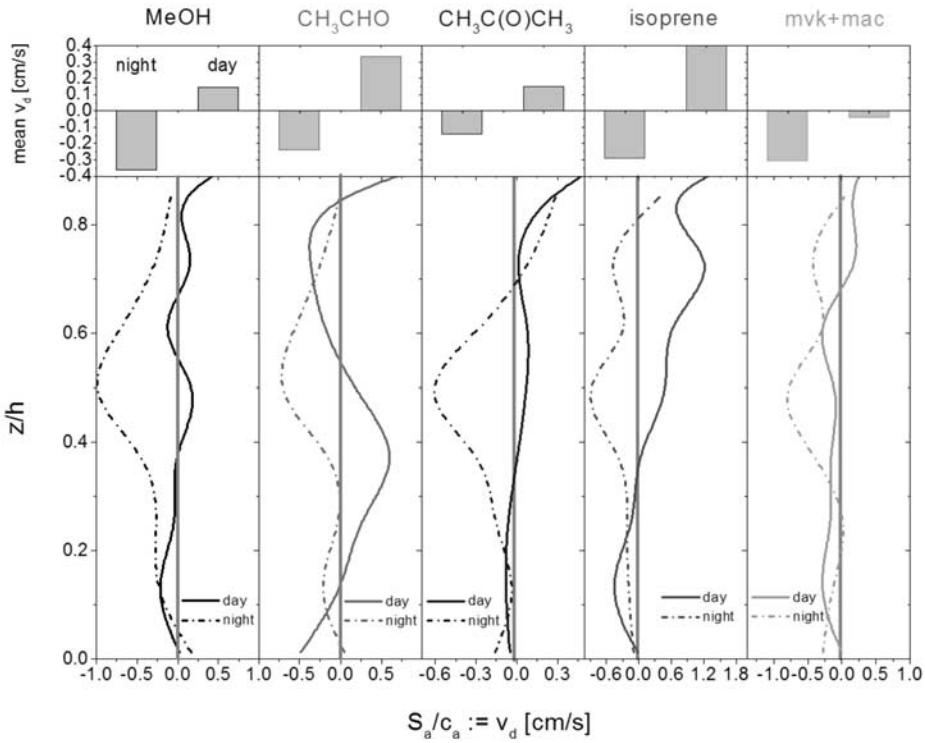

Figure 9. Source/sink layers, expressed as a flux rate (vd: = S_a/c_a), for methanol, acetaldehyde, acetone, isoprene, and MVK+MAC obtained from the dispersion calculation are plotted versus normalized height (z/h) and averaged over day (solid line) and night (dashed line). The top panels depict mean values for day and night. See color version of this figure at back of this issue.

according to v_d : = dC/C × 23 [m]/T [h] for T = 8–12 hours, with dC being the concentration drop and C the mean concentration. Within the uncertainty these deposition velocities (except for acetic and formic acid) are significantly larger (0.03–0.08 cm/s) than calculated according to standard procedures outlined by *Wesely* [1989]. However, for most compounds (methanol, acetone, acetonitrile, acetaldehyde, and MVK+MAC) the calculated deposition caused by dew can still at most only explain 35% of the observed deposition at La Selva. A more sophisticated formalism for the uptake of organics due to the formation of dew [*Chameides*, 1987] shows that for moderately soluble compounds (H = 15–220 M/atm), lifetimes τ between 10 and 300 s are required in the liquid phase. *Jayne et al.* [1992] measured uptake rates of formaldehyde and acetaldehyde. They found that despite its low hydration constant acetaldehyde is taken up by cloud droplets more efficiently than expected. According to their results we calculate deposition velocities for acetaldehyde of 0.03–0.20 cm/s at a pH between 5 and 3 due to hydrolysis. *Sanhueza et al.* [1992] measured a typical pH of 5.5 ± 0.5 above a tropical cloud forest during the wet season, which corresponds to a v_{dep} of 0.03. This value is lower than our observations but higher than the range predicted in atmospheric models. For example, high uptake rates of acetaldehyde have tentatively been confirmed by a modeling study of Los Angeles cloud chemistry data [*Seigneur and Wegrecki*, 1989]. The model underpredicted aqueous concentrations in cloud water by a factor of 40. Overall we conclude that the low canopy resistance (R_c) observed during this study can only partly be explained by the formation of dew, unless its formation happens under very acidic conditions (pH < 3). In this case, various organics could react more rapidly [*Noziere and Riemer*, 2003; *Voisin et al.*, 2004], resulting in a significant increase of their solubilities and effective Henry's law constants. On the other hand, the uptake of acetone by acidic solutions was reported to be minor [*Duncan et al.*, 1999].

[26] Assuming that 35% of the observed deposition is due to the formation of dew, the dissolved organics should potentially evaporate in the morning. The fact that we do not observe a significant emission pulse after sunrise suggests that evaporation is either minor or happens gradually. We hypothesize that part of the dissolved organics can probably also be taken up and metabolized by the vegetation itself or microbes on various surfaces and part might be lost in the soil as dewdrops fall to the ground. In any case the overall low canopy resistance (R_c) argues for a significant sink manifested by our nighttime observations. The potential sink of VOCs is scaled up for tropical ecosystems (17×10^6 km^2) taking mean daytime (column 2) and nighttime (column 3) concentrations and is listed in column 10 of Table 2.

[27] Acetic and formic acid, as well as MVK+MAC, were mainly deposited. Our deposition measurements for acetic and formic acid lie within the previously reported range above tropical forests [*Sanhueza et al.*, 1992; *Kuhn et al.*, 2002b]. On average the combined daytime deposition flux (velocity) of MVK+MAC is substantially lower during this study (average vd ~0.1 cm/s, see Figure 9) than fluxes

Table 2. Measured Ambient Concentrations C_a During Day and Night, Henry's Law Constant (H), Measured Deposition Velocity (vd), Canopy Resistance (R_c), Range of the Estimated Total Sink Due to Dry Deposition for Tropical Ecosystems Taking Mean Night and Daytime Concentrations (R1), Predicted Deposition Including Dew Formation According to *Wesely* [1989] (R2), Potential Deposition Velocity Based on Equation (3) and a Liquid Volume (Vl) Between 22 and 114 l, Loss Due to Chemical Losses (R3) Expressed as a Deposition Velocity (h/τ), and Estimated Sink (S)

Compound	C_a, ppbv 0600–1800	C_a, ppbv 1800–0600	H, M atm^{-1}	$V_{d,measured}$, cm s^{-1} 1800–0600	R_c, s m^{-1}	$V_d^{(R1)}$,[a] cm s^{-1}	$V_d^{(R2)}$,[b] cm s^{-1}	$V_d^{(R3)}$,[c] cm s^{-1}	S, Tg yr^{-1}
$1/(R_a + R_b)$				0.70 ± 0.15					
Acetic acid[d]	1.01	0.80	4000	0.15 ± 0.01	547	0.13	0.06–0.08	≪[e]	1.0–2.4
Formic acid[d]	1.30	0.51	9000	0.15 ± 0.09	512	0.13	0.06–0.08	≪	1.8–2.4
Methanol[f]	2.78	1.53	220	0.27 ± 0.14	231	0.02	0.05–0.08	3.3E-04	1.8–3.1
Acetone[f]	1.14	0.73	30	0.14 ± 0.01	582	0.02	0.04–0.06	8.0E-05	0.8–1.2
Acetonitrile[g]	0.27	0.10	49	0.19 ± 0.01	387	0.02	0.05–0.07	≪	0.2–0.5
Acetaldehyde[f]	0.44	0.26	15	0.26 ± 0.03	242	0.02	0.03–0.05	5.3E-03	0.4–0.7
Isoprene[f]	1.66	0.31	0.028	0.25 ± 0.05	250	0.02	≪	0.26	0.7–3.8
MVK+MAC[h]	0.88	0.12	41	0.45 ± 0.15	82	0.02	0.04–0.07	0.02	0.6–4.6

[a(R1)] *Wesely* [1989].
[b(R2)] Equation (4).
[c(R3)] Due to [O_3 + HO + NO_3] chemistry.
[d] Deposition scaled up for a full day using the listed deposition velocity.
[e] Not important.
[f] Assumed that dry deposition mainly occurs at nighttime due to daytime emissions and a potential compensation point.
[g] Here 0.16 cm/s used for daytime deposition of acetonitrile inferred from our measurements.
[h] Here 0.10 cm/s used for daytime deposition of MVK+MAC inferred from our measurements.

reported during LBA-EUSTACH. *Andreae and Merlet* [2001], for example, published a deposition flux of MAC+MVK of 118 ng m^{-2} s^{-1}. Taking typical ambient daytime concentration measurements of MAC+MVK on the order of 1–2 ppbv during LBA-EUSTACH [*Andreae et al.*, 2002; *Kesselmeier et al.*, 2002a], the deposition velocity observed in the Amazon would be as high as 2 to 4 cm/s, close to the aerodynamic limit.

[28] On the other hand, we observed substantial losses of most VOCs inferred from the mass balance equation as well as the inverse Lagrangian transport model during nighttime. The deposition of oxidation products from isoprene photochemistry has recently been identified as a significant uncertainty in a global modeling study by *von Kuhlmann et al.* [2003]. von Kuhlmann et al., however, mainly paid attention to the deposition of very soluble intermediates such as hydroxyhydro-peroxides. In the present study we also observe effective deposition of moderately soluble compounds, such as MVK+MAC. In order to reduce resulting discrepancies, other box and global chemistry models empirically assign deposition velocities up to 2.5 cm/s for isoprene [*Jacob and Wofsy*, 1988; *Wang et al.*, 1998]. *Hurst et al.* [2001] observed significant decay rates of isoprene after sunset and argued that deposition velocities of 1.5–2.0 cm/s for isoprene would be rather unrealistic. The authors hypothesized that mixing effects above heterogeneous terrain or nighttime HO could possibly explain these observations but could not constrain their assumptions accurately enough. Here we observe a comparable net loss of isoprene ($\tau \sim$ 2.5 h) which can be expressed as an apparent deposition velocity of 0.35 cm/s. Using the NCAR Master Mechanism constrained by measured VOC, ozone, and NO_x, we calculate potential NO_3 concentrations up to 4 pptv, which would be sufficiently high to explain most of the observed loss of isoprene during nighttime. The high deposition of oxygenated compounds (except organic acids) could not be explained by chemistry and only partly (up to 35%) by the formation of dew. Other possibilities such as the partitioning onto aerosols are largely unexplored; however, recent findings suggest that even compounds that were historically not thought to partition into the aerosol phase (e.g., isoprene) could be involved in heterogeneous reactions on acidic particles. Humic-like substances that account for a major identified fraction of organic aerosols are likely related to primary biogenic emissions and possibly various oxygenated VOCs [*Limbeck et al.*, 2003; *Jang and Kamens*, 2001; *Matsunaga et al.*, 2003].

[29] If our results can be generalized, the overall dry deposition to tropical forests (mean value from Table 2) is estimated to be 2.4, 1.1, 0.4, 0.54, and 2.0 Tg/yr for methanol, acetone, acetonitrile, acetaldehyde, and MVK+MAC, respectively. This amounts to 0.5–2.4% [*Heikes et al.*, 2002], 1.2%, 0.3% [*Singh et al.*, 2003], and 36% of the total global source strengths of methanol, acetone, acetaldehyde, and acetonitrile, respectively. For tropical ecoregions the measured deposition would be 6%, 5.5%, 3.4%, and 5% of the total net emission/production of methanol, acetone, acetaldehyde, and MVK+MAC, but could potentially add up to 25%, 13%, 8%, and 10%, respectively. The measured dry deposition to land for methanol is higher than that used for estimating the global budget [*Heikes et al.*, 2002], which was based on formic acid. Our finding suggests that the high deposition observed for compounds such as methanol is not necessarily only related to their solubility. The global source strength of acetonitrile has recently been extrapolated from biomass burning studies [*Holzinger et al.*, 1999], ambient observations of acetonitrile concentrations in the stratosphere [*Schneider et al.*, 1997], over the Pacific Ocean [*Singh et al.*, 2003], and a literature assessment [*Andreae and Merlet*, 2001; *Bange and Williams*, 2000]. These budget estimates range between 0.6 and 2.3 Tg yr^{-1}. From our results the estimated dry deposition to tropical rain forests alone would add up to 0.2 Tg yr^{-1}, which is ~20% of the estimated global dry deposition to oceans [*Singh et al.*, 2003]. Taking recent observations above the tropical savanna [*Sanhueza et*

al., 2003], it appears that high dry deposition to land is not only limited to dense vegetation. Assuming that dry deposition occurs at similar rates during dry and wet seasons with average deposition velocities of 0.14 cm/s for tropical grasslands/savannas [*Sanhueza et al.*, 2003] and 0.19 cm/s for tropical forests (this work) (total area: 32×10^6 km^2), the total sink would add up to 0.2–0.7 Tg yr^{-1}, comparable to the estimated uptake by oceans (1.2 Tg yr^{-1} [*Singh et al.*, 2003]). This in turn implies that the source strength of acetonitrile is most likely higher than the current best estimate of ~1.5 Tg yr^{-1}.

5. Conclusion

[30] On-line monitoring of a variety of biogenically and photochemically produced VOCs using a proton-transfer-reaction mass spectrometer provided new insights in the exchange processes above a tropical primary rain forest. Fluxes inferred from a continuous in-canopy profiling system in general agreed well with eddy covariance measurements performed at 10 m above the canopy. We used Lagrangian dispersion theory to infer the source/sink distributions of VOCs in the canopy. Isoprene emissions could be described by conventional parameterizations [e.g., *Guenther*, 1997]. In contrast with previous leaf-level measurements made at La Selva [*Geron et al.*, 2002], our observations revealed light-dependent monoterpene emissions. This implies that light-dependent monoterpene emissions, which have also been observed on the leaf and branch level in temperate and tropical forests [e.g., *Staudt and Seufert*, 1995; *Ciccioli et al.*, 1997; *Kuhn et al.*, 2002a] as well as on the canopy scale [*Rinne et al.*, 2002], are frequently found in tropical ecosystems. It also illustrates the complexity of VOC emissions from tropical ecosystems where previous screening of various tropical species did not reveal substantial monoterpene emissions [*Geron et al.*, 2002]. Considering the large species diversity in tropical forests, this is not entirely surprising. Whole-canopy studies can integrate over the entire ecosystem and can therefore reliably be used for upscaling net emissions in a representative manner.

[31] Methanol, acetone, and acetaldehyde were mainly emitted during daytime. Their fluxes followed a temperature-dependent pattern similar to that observed above other ecosystems [*Schade and Goldstein*, 2001; *Baker et al.*, 2001]. Using environmental data from the year 1999, we estimate that up to 5.5% of the eddy-covariance estimate for NEE [*Loescher et al.*, 2003] can be emitted in the form of methanol, acetaldehyde, acetone, isoprene, and monoterpenes. From these data we infer a significant source strength for tropical ecosystems on the order of 36, 16, 19, 106, and 7 Tg/yr for methanol, acetaldehyde, acetone, isoprene, and monoterpenes. The total emission estimate for these compounds ranges between 120 and 250 Tg/yr. The total estimate for isoprene emissions is a factor of 3–4 lower than that inferred by *Guenther et al.* [1995]. This is not entirely surprising since we expect significant spatial variability and seasonally driven changes in ecosystem function. Previous dry season studies in the Congo and Amazon tropical forests have reported isoprene fluxes that are of a similar magnitude [e.g., *Rinne et al.*, 2002; *Serca et al.*, 2001] or higher [e.g., *Helmig et al.*, 1998; *Zimmerman et al.*, 1988; *Rasmussen and Khalil*, 1988]. Comparing these canopy scale observations, it appears that there is a seasonal emission variability of a factor of 2–3 and a spatial emission variability of a factor of 3–4. In order to obtain better accuracy for bottom-up approaches the spatial and temporal variation of isoprene emissions in tropical regions needs to be investigated based on long-term flux measurements such as those performed at sites in the United States [*Schade and Goldstein*, 2002; *Westberg et al.*, 2001] as well as airborne flux measurements.

[32] Our observations raise the possibility that dry deposition of VOCs above dense vegetation might currently be substantially underestimated. Tropical ecosystems therefore do not only play an important role as source regions for many VOCs but can have the capability to filter and effectively recapture part of the emitted and photochemically produced compounds. Recycling of VOCs might therefore dampen the impact of surface emissions on boundary layer chemistry. In this connection, tropical ecosystems contrast arctic regions, which are characterized by a very active atmospheric chemistry above snowpacks due to the effective revolatilization of ozone/HO_x/NO_x precursors [*Shepson et al.*, 2003]. However, at this point too little is known in order to relate our observations to ecosystem function and various other variables controlling VOC exchange patterns in and above other forested areas.

[33] We conclude that flux measurements in the surface layer are crucial for understanding the cycling and fate of reactive carbon. On-line monitoring by proton-transfer-reaction mass spectrometry proves to be a valuable tool for biogeochemical flux measurements of reactive carbon. In order to improve our understanding of exchange processes at the surface, future experiments will need to aim at seasonal and airborne flux studies. These experiments will represent an important link between bottom-up and top-down approaches. Improved surface emission models of VOCs will subsequently lead to a better predictive capability of atmospheric chemistry models.

Appendix A

A1. Numerical Calculation of the Dispersion Matrix According to *Raupach* [1986a, 1986b] and *Nemitz et al.* [2000]

[34] Equation (3) can be rewritten in nonvector form:

$$c_i - c_{ref} = \sum_{j=1}^{m} d_{i,j} \cdot S_j. \quad (A1)$$

In order to account for a limited number of source and concentrations layers we follow the strategy outlined by *Nemitz et al.* [2000], who subdivide each concentration (z^c) and source (z^s) layer into r sublayers. The ILT approach proposed by *Raupach* [1986a, 1986b] divides the overall transport in two terms, a "near field" and "far field" term. The matrix elements of the near field term α_{ij} (accounting

for near field effects as described by *Raupach* [1986a, 1986b]) are given by

$$\alpha_{ij} = \frac{\delta z_j^s}{r} \cdot \sum_{l=1}^{r} \frac{k_n(x) + k_n(y)}{\sigma_w\left(z_{jl}^s\right)},$$

$$k_n(u) = -\frac{1}{\sqrt{2\pi}} \cdot \ln(1 - e^{-u}) + \frac{0.5 - \pi^2}{6\sqrt{2\pi}} \cdot e^{-u} \tag{A2}$$

$$x := \frac{z_i^c - z_{jl}^s}{\sigma_w\left(z_{jl}^s\right) \cdot T_L\left(z_{jl}^s\right)},$$

$$y := \frac{z_i^c + z_{jl}^s}{\sigma_w\left(z_{jl}^s\right) \cdot T_L\left(z_{jl}^s\right)}.$$

The "near-field kernel" function $k_n(u)$ is a numerical approximation derived by *Raupach* [1986a, 1986b], δz_j^s is the distance between the individual source layers, $\sigma_w(z)$ is the standard deviation of the vertical wind velocity at height z according to 1a, $T_L(z)$ is the Lagrangian timescale at height z according to 1b, z_i^c is the concentration height at index i, and z_i^s is the source height at index j. The index l runs from 1 to r, representing r sublayers for the source terms.

[35] The matrix elements of the far field (diffusive) term β_{ij} are similarly subdivided and given by

$$\beta_{ij} = \frac{z_{ref} - z_i}{s_i} \sum_{k=1}^{s_i} b_{ijk},$$

$$s_i = r \cdot (n + 1 - i), with\ i = 1 - n, j = 1 - m$$

$$b_{ijk} = \begin{cases} 0, & z_{ik}^c \le z_{j-1}^s \\ \left(z_{ik}^c - z_{j-1}^s\right) / \left(\sigma_w^2\left(z_{ik}^c\right) \cdot T_L\left(z_{ik}^c\right)\right), & z_{j-1}^s \le z_{ik}^c \le z_j^s, \\ \delta z_j^s / \sigma_w^2\left(z_{ik}^c\right) \cdot T_L\left(z_{ik}^c\right) & z_{ik}^c > z_j^s \end{cases} \tag{A3}$$

where z_{ref} is the reference height of the concentration measurement (uppermost sampling height above or just at the height of the canopy h) and z_i is the height at index i of the concentration vector. The individual terms α_{ij} and β_{ij} are subsequently combined to give the total dispersion matrix

$$\left(d_{ij}\right) : d_{ij} = \alpha_{ij} - \alpha_{n+1,j} + \beta_{ij}. \tag{A4}$$

A2. Numerical Calculation of the Dispersion Matrix According to *Warland and Thurtell* [2000]

[36] *Warland and Thurtell* [2000] have recently presented a continuous solution of the Lagrangian dispersion problem [*Taylor*, 1921] and define a dispersion matrix d_{ij} such that,

$$\left.\frac{dc}{dz}\right|_i = \sum_{j=1}^{m} d_{ij} S_j, \tag{A5}$$

where S_j is the source strength at index (height) j and $dc/dz|_i$ is the local concentration gradient at index i. The dispersion matrix d_{ij} is given by

$$d_{ij} = \left\{ \frac{-\left[1 - \exp\left(\frac{-(z_i - z_j)^2}{2\Delta z_j^2}\right)\right]}{2\sigma_w^2(z_i) \cdot T_L(z_i) \cdot \left[1 - \exp\left(-\sqrt{\frac{\pi}{2}} \frac{(z_i - z_j)}{[\sigma_w(z_i) \cdot T_l(z_i) + \sigma_w(z_j) \cdot T_l(z_j)]/2}\right)\right]} - \frac{\left[1 - \exp\left(\frac{-(z_i + z_j)^2}{2\Delta z_j^2}\right)\right]}{2\sigma_w^2(z_i) \cdot T_L(z_i) \cdot \left[1 - \exp\left(-\sqrt{\frac{\pi}{2}} \frac{(z_i + z_j)}{[\sigma_w(z_i) \cdot T_l(z_i) + \sigma_w(z_j) \cdot T_l(z_j)]/2}\right)\right]} \right\}, \text{ for } z_i > z_j,$$

$$d_{ij} = \left\{ \frac{-\left[1 - \exp\left(\frac{-(z_i + z_j)^2}{2\Delta z_j^2}\right)\right]}{2\sigma_w^2(z_i) \cdot T_L(z_i) \cdot \left[1 - \exp\left(-\sqrt{\frac{\pi}{2}} \frac{(z_j + z_i)}{[\sigma_w(z_i) \cdot T_l(z_i) + \sigma_w(z_j) \cdot T_l(z_j)]/2}\right)\right]} \right\}, \text{ for } z_i = z_j \text{ and}$$

$$d_{ij} = \left\{ \frac{\left[1 - \exp\left(\frac{-(z_i - z_j)^2}{2\Delta z_j^2}\right)\right]}{2\sigma_w^2(z_i) \cdot T_L(z_i) \cdot \left[1 - \exp\left(-\sqrt{\frac{\pi}{2}} \frac{(z_j - z_i)}{[\sigma_w(z_i) \cdot T_l(z_i) + \sigma_w(z_j) \cdot T_l(z_j)]/2}\right)\right]} - \frac{\left[1 - \exp\left(\frac{-(z_i + z_j)^2}{2\Delta z_j^2}\right)\right]}{2\sigma_w^2(z_i) \cdot T_L(z_i) \cdot \left[1 - \exp\left(-\sqrt{\frac{\pi}{2}} \frac{(z_i + z_j)}{[\sigma_w(z_i) \cdot T_l(z_i) + \sigma_w(z_j) \cdot T_l(z_j)]/2}\right)\right]} \right\}, \text{ for } z_i < z_j. \tag{A6}$$

A3. Random Walk Model Adopted From CANVEG

[37] The CANVEG random walk model calculates particle trajectories as described by *Raupach* [1986b], where the particle position (X(t), Z(t)) and streamwise velocity components (U(t), W(t)) evolve according to

$$\begin{pmatrix} d\left(\frac{W}{\sigma_w(Z,t)}\right) \\ dZ \\ U \\ dX \end{pmatrix} = \begin{pmatrix} \frac{Wdt}{\sigma_w(Z,t) \cdot T_L(Z,t)} + d\Omega(Z,t) \\ Wdt \\ \overline{u}(Z) \\ Udt \end{pmatrix}, \tag{A7}$$

with $d\Omega(Z, t)$ being a random force acting on the moving particle. Based on equation (A7) the random walk module of CANVEG (http://nature.berkeley.edu/biometlab/) can be used to calculate a dispersion matrix d_{ij}.

[38] **Acknowledgments.** We are grateful to Steven Oberbauer and Henry Loescher for providing environmental data for La Selva, to Eiko Nemitz for helpful discussions about the inverse Lagrangian transport model, and to Dennis Baldocchi for providing a new C^{++} version of the random walk model subroutine used in the CANVEG model. We also thank the Organization for Tropical Studies and Jed Sparks for supplying logistical support. The National Center for Atmospheric Research is sponsored by the National Science Foundation. This work was also in part supported by NSF grant ATM- 0119995.

References

Andreae, M. O., and P. J. Crutzen (1997), Atmospheric aerosols: Biogeochemical sources and role in atmospheric chemistry, *Science*, *276*, 1052–1058.

Andreae, M. O., and P. Merlet (2001), Emissions of trace gases and aerosols from biomass burning, *Global Biogeochem. Cycles*, *15*(4), 955–966.

Andreae, M. O., et al. (2002), Biogeochemical cycling of carbon, water, energy, trace gases, and aerosols in Amazonia: The LBA-EUSTACH experiments, *J. Geophys. Res.*, *107*(D20), 8066, doi:10.1029/2001JD000524.

Baker, B., A. Guenther, J. Greenberg, and R. Fall (2001), Canopy level fluxes of 2-metyl-3-buten-2-ol, acetone, and methanol by a portable relaxed eddy accumulation system, *Environ. Sci. Technol.*, *35*, 1701–1708.

Baldocchi, D. D., B. B. Hicks, and P. Camara (1987), A canopy stomatal resistance model for gaseous deposition to vegetated surfaces, *Atmos. Environ.*, *21*, 91–101.

Bange, H. W., and J. Williams (2000), New directions: Acetonitrile in the atmosphere and biogeochemical cycles, *Atmos. Environ.*, *34*, 4959–4960.

Barth, M., et al. (2004), Future scientific directions: Coupling between land ecosystems and the atmospheric hydrologic cycle through biogenic aerosol pathways, *Bull. Am. Meteorol. Soc.*, in press.

Chameides, W. L. (1987), Acid dew and the role of chemistry in the dry deposition of reactive gases to wetted surfaces, *J. Geophys. Res.*, *92*, 11,895–11,908.

Ciccioli, P., C. Fabozzi, and E. Brancaleoni (1997), Use of the isoprene algorithm for predicting the monoterpene emission from the Mediterranean holm oak Quercus ilex L: Performance and limits of this approach, *J. Geophys. Res.*, *102*, 23,319–23,328.

Clark, D. A., S. Brown, D. Kicklighter, J. Chambers, J. R. Thomlinson, J. Ni, and E. A. Holland (2001), NPP in tropical forests: An evaluation and synthesis of existing field data, *Ecol. Appl.*, *11*, 371–384.

Clark, D. B., and D. A. Clark (2000), Landscape-scale variation in forest structure and biomass in a tropical rain forest, *For. Ecol. Manage.*, *137*, 185–198.

Clark, D. B., D. A. Clark, P. M. Rich, S. Weiss, and S. F. Oberbauer (1996), Landscape-scale distribution of understory light and forest structure in a neotropical lowland rain forest, *Can. J. For. Res.*, *26*, 747–757.

Cleveland, C. C., and J. B. Yavitt (1997), Consumption of atmospheric isoprene in soil, *Geophys. Res. Lett.*, *24*, 2379–2382.

Cojocariu, C., J. Kreuzwieser, and H. Rennenberg (2004), Correlation of short-chained carbonyls emitted from Picea abies with physiological and environmental parameters, *New Phytol.*, *162*, 717–727.

Collins, W. J., R. G. Derwent, C. E. Johnson, and D. S. Stevenson (2002), The oxidation of organic compounds in the troposphere and their global warming potentials, *Clim. Change*, *52*, 453–479.

Cox, P. M., R. A. Betts, C. D. Jones, S. A. Spall, and I. J. Totterdell (2000), Acceleration of global warming due to carbon-cycle feedbacks in a coupled climate model, *Nature*, *408*, 184–187.

Crutzen, P. J., et al. (2000), High spatial and temporal resolution measurements of primary organics and their oxidation products over the tropical forests of Surinam, *Atmos. Environ.*, *34*, 1161–1165.

Curtis, P. S., P. J. Hanson, P. Bolstad, C. Barford, J. C. Randolph, H. P. Schmid, and K. B. Wilson (2002), Biometric and eddy-covariance based estimates of annual carbon storage in five eastern North American deciduous forests, *Agric. For. Meteorol.*, *113*, 3–19.

de Gouw, J., C. Warneke, T. Karl, G. Eerdekens, C. van der Veen, and R. Fall (2003a), Sensitivity and specificity of atmospheric trace gas detection by Proton-Transfer-Reaction Mass Spectrometry, *Int. J. Mass Spectrom.*, *223*, 365–382.

de Gouw, J. A., P. D. Goldan, C. Warneke, W. C. Kuster, J. M. Roberts, M. Marchewka, S. B. Bertman, A. A. P. Pszenny, and W. C. Keene (2003b), Validation of proton transfer reaction-mass spectrometry (PTR-MS) measurements of gas-phase organic compounds in the atmosphere during the New England Air Quality Study (NEAQS) in 2002, *J. Geophys. Res.*, *108*(D21), 4682, doi:10.1029/2003JD003863.

Duncan, J. L., L. R. Schindler, and J. T. Roberts (1999), Chemistry at and near the surface of liquid sulfuric acid: A kinetic, thermodynamic, and mechanistic analysis of heterogeneous reactions of acetone, *J. Phys. Chem. B*, *103*, 7247–7259.

Fall, R. (2003), Abundant oxygenated in the atmosphere: A biochemical perspective, *Chem. Rev.*, *103*, 4941–4951.

Fall, R., T. Karl, A. Hansel, A. Jordan, and W. Lindinger (1999), Volatile organic compounds emitted after leaf wounding: On-line analysis by proton-transfer-reaction mass spectrometry, *J. Geophys. Res.*, *104*, 15,963–15,974.

Fitzjarrald, D. R., and K. E. Moore (1990), Mechanisms of nocturnal exchange between the rain forest and the atmosphere, *J. Geophys. Res.*, *95*, 16,839–16,850.

Galbally, I. E., and W. Kirstine (2002), The production of methanol by flowering plants and the global cycle of methanol, *J. Atmos. Chem.*, *43*, 195–229.

Geron, C., A. Guenther, J. Greenberg, H. W. Loescher, D. Clark, and B. Baker (2002), Biogenic volatile organic compound emissions from a lowland tropical wet forest in Costa Rica, *Atmos. Environ.*, 3793–3802.

Golley, F. B., and G. S. Hartshorn (1984), Tropical rain forest ecosystems—Structure and function, *Ecology*, *65*, 334–335.

Greenberg, J. P., and P. R. Zimmerman (1984), Nonmethane hydrocarbons in remote tropical, continental, and marine atmospheres, *J. Geophys. Res.*, *89*, 4767–4778.

Guenther, A. (1997), Seasonal and spatial variations in natural volatile organic compound emissions, *Ecol. Appl.*, *7*, 34–45.

Guenther, A., et al. (1995), A global model of natural volatile organic compound emissions, *J. Geophys. Res.*, *100*, 8873–8892.

Harley, P., A. Guenther, and P. Zimmerman (1997), Environmental controls over isoprene emission in deciduous oak canopies, *Tree Physiol.*, *17*, 705–714.

Harley, P., et al. (2004), Variation in potential for isoprene emissions among Neotropical forest sites, *Global Change Biol.*, *10*, doi:10.1111/j.1529-8817.2003.00760.x.

Heikes, B. G., et al. (2002), Atmospheric methanol budget and ocean implication, *Global Biogeochem. Cycles*, *16*(4), 1133, doi:10.1029/2002GB001895.

Helmig, D., B. Balsley, K. Davis, L. R. Kuck, M. Jensen, J. Bognar, T. Smith, R. V. Arrieta, R. Rodriguez, and J. W. Birks (1998), Vertical profiling and determination of landscape fluxes of biogenic nonmethane hydrocarbons within the planetary boundary layer in the Peruvian Amazon, *J. Geophys. Res.*, *103*, 25,519–25,532.

Holzinger, R., C. Warneke, A. Hansel, A. Jordan, W. Lindinger, D. H. Scharffe, G. Schade, and P. J. Crutzen (1999), Biomass burning as a source of formaldehyde, acetaldehyde, methanol, acetone, acetonitrile, and hydrogen cyanide, *Geophys. Res. Lett.*, *26*, 1161–1164.

Holzinger, R., L. Sandoval-Soto, S. Rottenberger, P. J. Crutzen, and J. Kesselmeier (2000), Emissions of VOCs from Quercus ilex L. measured by PTR-MS under different environmental conditions, *J. Geophys. Res.*, *105*, 20,573–20,579.

Horst, T. W., and J. C. Weil (1992), Footprint estimation for scalar flux measurements in the atmospheric surface layer, *Boundary Layer Meteorol.*, *59*, 279–296.

Hurst, J. M., et al. (2001), Investigation of the nighttime decay of isoprene, *J. Geophys. Res.*, *106*, 24,335–24,346.

Jacob, D. J., and S. C. Wofsy (1988), Photochemistry of biogenic emissions over the Amazon forest, *J. Geophys. Res.*, *93*, 1477–1486.

Jang, M., and R. M. Kamens (2001), Atmospheric secondary aerosol formation by heterogeneous reactions of aldehydes in the presence of a sulfuric acid aerosol catalyst, *Environ. Sci. Technol.*, *35*, 4758–4766.

Jayne, J. T., S. X. Duan, P. Davidovits, D. R. Worsnop, M. S. Zahniser, and C. E. Kolb (1992), Uptake of gas-phase aldehydes by water surfaces, *J. Phys. Chem.*, *96*, 5452–5460.

Karl, T., A. Guenther, C. Lindinger, A. Jordan, R. Fall, and W. Lindinger (2001), Eddy covariance measurements of oxygenated VOC fluxes from crop harvesting using a redesigned proton-transfer-reaction mass spectrometer, *J. Geophys. Res.*, *106*, 24,157–24,167.

Karl, T., C. Spirig, P. Prevost, C. Stroud, J. Rinne, J. Greenberg, R. Fall, and A. Guenther (2002a), Virtual disjunct eddy covariance measurements of organic compound fluxes from a subalpine forest using proton transfer reaction mass spectrometry, *Atmos. Chem. Phys.*, *2*, 279–291.

Karl, T., A. Curtis, T. Rosenstiel, R. Monson, and R. Fall (2002b), Transient releases of acetaldehyde from tree leaves—Products of a pyruvate overflow mechanism?, *Plant Cell Environ.*, *25*, 1121–1131.

Karl, T., A. Guenther, C. Spirig, A. Hansel, and R. Fall (2003), Seasonal variation of biogenic VOC emissions above a mixed hardwood forest in northern Michigan, *Geophys. Res. Lett.*, *30*(23), 2186, doi:10.1029/2003GL018432.

Kesselmeier, J., et al. (2002a), Concentrations and species composition of atmospheric volatile organic compounds (VOCs) as observed during the wet and dry season in Rondonia (Amazonia), *J. Geophys. Res.*, *107*(D20), 8053, doi:10.1029/2000JD000267.

Kesselmeier, J., et al. (2002b), Volatile organic compound emissions in relation to plant carbon fixation and the terrestrial carbon budget, *Global Biogeochem. Cycles*, *16*(4), 1126, doi:10.1029/2001GB001813.

Kreuzwieser, J., F. Kühnemann, A. Martis, H. Rennenberg, and W. Urbau (2000), Diurnal pattern of acetaldehyde emission by flooded poplar trees, *Plant Physiol.*, *108*, 79–86.

Kuhn, U., S. Rottenberger, T. Biesenthal, A. Wolf, G. Schebeske, P. Ciccioli, E. Brancaleoni, M. Frattoni, T. M. Tavares, and J. Kesselmeier (2002a), Isoprene and monoterpene emissions of Amazonian tree species during the wet season: Direct and indirect investigations on controlling environmental functions, *J. Geophys. Res.*, *107*(D20), 8071, doi:10.1029/2001JD000978.

Kuhn, U., S. Rottenberger, T. Biesenthal, C. Ammann, A. Wolf, G. Schebeske, S. T. Oliva, T. M. Tavares, and J. Kesselmeier (2002b), Exchange of short-chain monocarboxylic acids by vegetation at a remote tropical forest site in Amazonia, *J. Geophys. Res.*, *107*(D20), 8069, doi:10.1029/2000JD000303.

Kuster, W. C., B. T. Jobson, T. Karl, D. Riemer, E. Apel, P. D. Goldan, and F. C. Fehsenfeld (2004), Intercomparison of volatile organic carbon measurement techniques and data at La Porte during the TexAQS2000 Air Quality Study, *Environ. Sci. Technol.*, *38*, 221–228.

Limbeck, A., M. Kulmala, and H. Puxbaum (2003), Secondary organic aerosol formation in the atmosphere via heterogeneous reaction of gaseous isoprene on acidic particles, *Geophys. Res. Lett.*, *30*(19), 1996, doi:10.1029/2003GL017738.

Lindinger, W., A. Hansel, and A. Jordan (1998), On-line monitoring of volatile organic compounds at pptv levels by means of proton-transfer-reaction mass spectrometry (PTRMS)—Medical applications, food control, and environmental research, *Int. J. Mass Spectrom.*, 191–241.

Litvak, M. E., S. Madronich, and R. K. Monson (1999), Herbivore-induced monoterpene emissions from coniferous forests: Potential impact on local tropospheric chemistry, *Ecol. Appl.*, *9*, 1147–1159.

Loescher, H. W., S. F. Oberbauer, H. L. Gholz, and D. B. Clark (2003), Environmental controls on net ecosystem-level carbon exchange and productivity in a Central American tropical wet forest, *Global Change Biol.*, *9*, 396–412.

Loescher, H. W., J. A. Bentz, S. F. Oberbauer, T. K. Ghosh, R. V. Tompson, and S. K. Loyalka (2004), Characterization and dry deposition of carbonaceous aerosols in a wet tropical forest canopy, *J. Geophys. Res.*, *109*, D02309, doi:10.1029/2002JD003353.

Madronich, S., and J. G. Calvert (1989), The NCAR master mechanism of gas phase chemistry—Version 2.0, *NCAR Tech. Note NCAR/TN-333+STR*, Natl. Cent. for Atmos. Res., Boulder, Colo.

Malhi, Y., D. D. Baldocchi, and P. G. Jarvis (1999), The carbon balance of tropical, temperate, and boreal forests, *Plant Cell Environ.*, *22*, 715–740.

Matsunaga, S., M. Mochida, and K. Kawamura (2003), Growth of organic aerosols by biogenic semivolatile carbonyls in the forestal atmosphere, *Atmos. Environ.*, *37*, 2045–2050.

McKeen, S. A., T. Gierczak, J. B. Burkholder, P. O. Wennberg, T. F. Hanisco, E. R. Keim, R. S. Gao, S. C. Liu, A. R. Ravis-hankara, and D. W. Fahey (1997), The photochemistry of acetone in the upper troposphere: A source of odd-hydrogen radicals, *Geophys. Res. Lett.*, *24*, 3177–3180.

Nemitz, E., M. A. Sutton, A. Gut, R. S. Jose, S. Husted, and J. K. Schjoerring (2000), Sources and sinks of ammonia within an oilseed rape canopy, *Agric. For. Meteorol.*, *105*, 385–404.

Noziere, B., and D. D. Riemer (2003), The chemical processing of gas-phase carbonyl compounds by sulfuric acid aerosols-2,4 pentanedione, *Atmos. Environ.*, *37*, 841–851.

Ozanne, C. M. P., et al. (2003), Biodiversity meets the atmosphere: A global view of forest canopies, *Science*, *301*, 183–186.

Pierson, W. R., W. W. Brachaczek, R. A. Gorse, S. M. Japar, and J. M. Norbeck (1986), On the acidity of dew, *J. Geophys. Res.*, *91*, 4083–4096.

Poeschl, U., et al. (2001), High acetone concentrations throughout the 0–12 km altitude range over the tropical rain forest in Surinam, *J. Atmos. Chem.*, *38*, 115–132.

Rasmussen, R. A., and M. A. K. Khalil (1988), Isoprene over the Amazon Basin, *J. Geophys. Res.*, *93*, 1417–1421.

Raupach, M. R. (1986a), Applying Lagrangian fluid mechanics to infer scalar source distributions from concentration profiles in plant canopies, *Agric. For. Meteorol.*, *47*, 85–108.

Raupach, M. R. (1986b), A practical Lagrangian method for relating scalar concentrations to source distributions in vegetation canopies, *Auart. J. R. Meteorol. Soc.*, *115*, 609–632.

Rinne, H. J. I., A. B. Guenther, C. Warneke, J. A. de Gouw, and S. L. Luxembourg (2001), Disjunct eddy covariance technique for trace gas flux measurements, *Geophys. Res. Lett.*, *28*, 3139–3142.

Rinne, H. J. I., A. B. Guenther, J. P. Greenberg, and P. C. Harley (2002), Isoprene and monoterpene fluxes measured above Amazonian rain forest and their dependence on light and temperature, *Atmos. Environ.*, *36*, 2421–2426.

Roberts, J. M., F. Flocke, C. A. Stroud, D. Hereid, E. Williams, F. Fehsenfeld, W. Brune, M. Martinez, and H. Harder (2002), Ground-based measurements of peroxycarboxylic nitric anhydrides (PANs) during the 1999 Southern Oxidants Study Nashville Intensive, *J. Geophys. Res.*, *107*(D21), 4554, doi:10.1029/2001JD000947.

Saleska, S. R., et al. (2003), Carbon in Amazon forests: Unexpected seasonal fluxes and disturbance-induced losses, *Science*, *302*, 1554–1557.

Sanhueza, E., M. Santana, and M. Hermoso (1992), Gas- and aqueous-phase formic and acetic acids at a tropical cloud forest site, *Atmos. Environ.*, *26*, 1421–1426.

Sanhueza, E., R. Holzinger, B. Kleiss, L. Donoso, and P. J. Crutzen (2003), New insights in the global cycle of acetonitrile: Release from the ocean and dry deposition in the tropical savanna of Venezuela, *Atmos. Chem. Phys. Discuss.*, *3*, 5275–5288.

Schade, G. W., and A. H. Goldstein (2001), Fluxes of oxygenated volatile organic compounds from a ponderosa pine plantation, *J. Geophys. Res.*, *106*, 3111–3123.

Schade, G. W., and A. H. Goldstein (2002), Plant physiological influences on the fluxes of oxygenated volatile organic compounds from ponderosa pine trees, *J. Geophys. Res.*, *107*(D10), 4082, doi:10.1029/2001JD000532.

Schneider, J., V. Buerger, and F. Arnold (1997), Methyl cyanide and hydrogen cyanide measurements in the lower stratosphere: Implications for methyl cyanide sources and sinks, *J. Geophys. Res.*, *102*, 25,501–25,506.

Schnitzler, J. P., et al. (2002), Emission of biogenic volatile organic compounds: An overview of field, laboratory, and modeling studies performed during the 'tropospheric teresach program,' TFS 1997–2000, *J. Atmos. Chem.*, *42*, 159–177.

Seigneur, C., and A. M. Wegrecki (1989), Mathematical-modeling of cloud chemistry in the Los Angeles basin, *Atmos. Environ.*, *24*, 989–1006.

Serca, D., et al. (2001), EXPRESSO flux measurements at upland and lowland Congo tropical forest sites, *Tellus*, *Ser. B*, *53*, 220–234.

Shepson, P., P. Matrai, L. Barrie, and J. Bottenheim (2003), Ocean-atmosphere-sea ice-snowpack interactions in the Arctic, and global change, *Eos Trans. AGU*, *84*(36), 349–355.

Singh, H. B., et al. (2003), In situ measurements of HCN and CH_3CN over the Pacific Ocean: Sources, sinks, and budgets, *J. Geophys. Res.*, *108*(D20), 8795, doi:10.1029/2002JD003006.

Siqueira, M., G. Katul, and C. T. Lai (2002), Quantifying net ecosystem exchange by multilevel ecophysiological and turbulent transport models, *Adv. Water Resour.*, *25*, 1357–1366.

Staudt, M., and G. Seufert (1995), Light-dependent emission of monoterpenes by holm oak (Quercus-Ilex L.), *Naturwissenschaften*, *82*, 89–92.

Steffen, W. L., and O. T. Denmead (Eds.) (1988), *Flow and Transport in the Natural Environment: Advances and Applications*, pp. 95–127, Springer-Verlag, New York.

Taylor, G. I. (1921), Diffusion by continuous movements, *Proc. London Math. Soc.*, Ser. 2, *20*, 196–211.

Trainer, M., E. J. Williams, D. D. Parrish, M. P. Buhr, E. J. Allwine, H. H. Westberg, F. C. Fehsenfeld, and S. C. Liu (1987), Models and observations of the impact of natural hydrocarbons on rural ozone, *Nature*, *329*, 705.

Voisin, D., B. Noziere, C. E. Longfellow, B. E. Henry, and D. R. Hanson (2004), Chemical processing of gas-phase methyl vinyl ketone, methacroleine, and 2-methyl-3-butene-2-ol by aqueous sulfuric acid: Implication for the troposphere, *J. Phys. Chem. A*, in press.

von Kuhlmann, R., M. G. Lawrence, U. Poeschl, and P. J. Crutzen (2003), Sensitivities in global scale modeling of isoprene, *Atmos. Chem. Phys. Discuss.*, *3*, 3095–3134.

Wang, Y. H., D. J. Jacob, and J. A. Logan (1998), Global simulation of tropospheric O_3-NO_x-hydrocarbon chemistry: 1. Model formulation, *J. Geophys. Res.*, *103*, 10,713–10,725.

Warland, J. S., and G. W. Thurtell (2000), A Lagrangian solution to the relationship between a distributed source and concentration profile, *Boundary Layer Meteorol.*, *96*, 453–471.

Warneke, C., S. L. Luxembourg, J. A. de Gouw, H. J. I. Rinne, A. B. Guenther, and R. Fall (2002), Disjunct eddy covariance measurements of oxygenated volatile organic compounds fluxes from an alfalfa field before and after cutting, *J. Geophys. Res.*, *107*(D8), 4067, doi:10.1029/2001JD000594.

Warneke, C., J. A. de Gouw, W. C. Kuster, P. D. Goldan, and R. Fall (2003), Validation of atmospheric VOC measurements by PTR-MS using a gas-chromatographic preseparation method, *Environ. Sci. Technol.*, *37*, 2494–2501.

Wesely, M. L. (1989), Parameterization of surface resistances to gaseous dry deposition in regional-scale numerical models, *Atmos. Environ.*, *23*, 1293–1304.

Westberg, H., B. Lamb, R. Hafer, A. Hills, P. Shepson, and C. Vogel (2001), Measurement of isoprene fluxes at the PROPHET site, *J. Geophys. Res.*, *106*, 24,347–24,358.

Wilson, J. D., and T. K. Flesch (1993), Flow boundaries in random-flight dispersion models: Enforcing the well-mixed condition, *J. Appl. Meteorol.*, *32*, 1695–1707.

Woodwell, G. M., and W. R. Dykeman (1966), Respiration of a forest measured by carbon dioxide accumulation during temperature inversions, *Science*, *154*, 1031–1034.

Zimmerman, P. R., J. P. Greenberg, and C. E. Westberg (1988), Measurements of atmospheric hydrocarbons and biogenic emission fluxes in the Amazon Boundary Layer, *J. Geophys. Res.*, *93*, 1407–1416.

D. Clark, Department of Biology, University of Missouri at St. Louis, 8001 Natural Bridge Rd., St. Louis, MO 62121, USA.

C. Geron, J. D. Herrick, and J. Walker, National Risk Management Research Laboratory, U.S. Environmental Protection Agency, Research Triangle Park, NC 27711, USA.

A. Guenther and T. Karl, Atmospheric Chemistry Division, National Center for Atmospheric Research, P.O. Box 3000, Boulder, CO 80307, USA. (tomkarl@ucar.edu)

M. Potosnak, Desert Research Institute, Reno, NV 89512, USA.

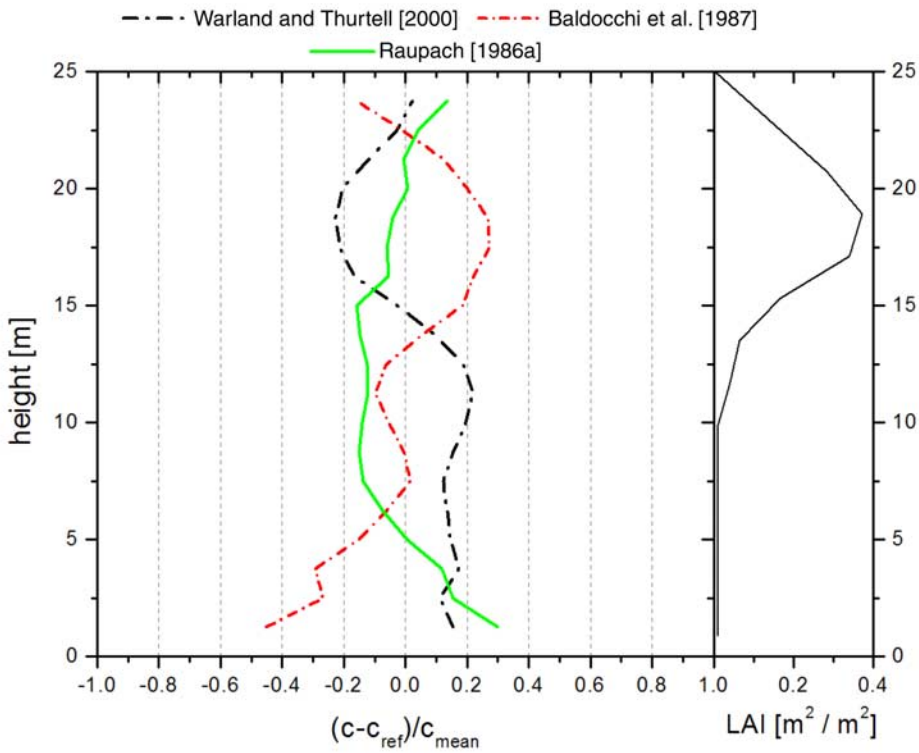

Figure 1. Comparison of the calculated concentrations between the LNF [*Raupach*, 1986a], the CNF [*Warland and Thurtell*, 2000], and the random walk [*Baldocchi et al.*, 1987] models, based on a given source profile following the LAI profile shown on the right side and expressed as a relative deviation from the mean.

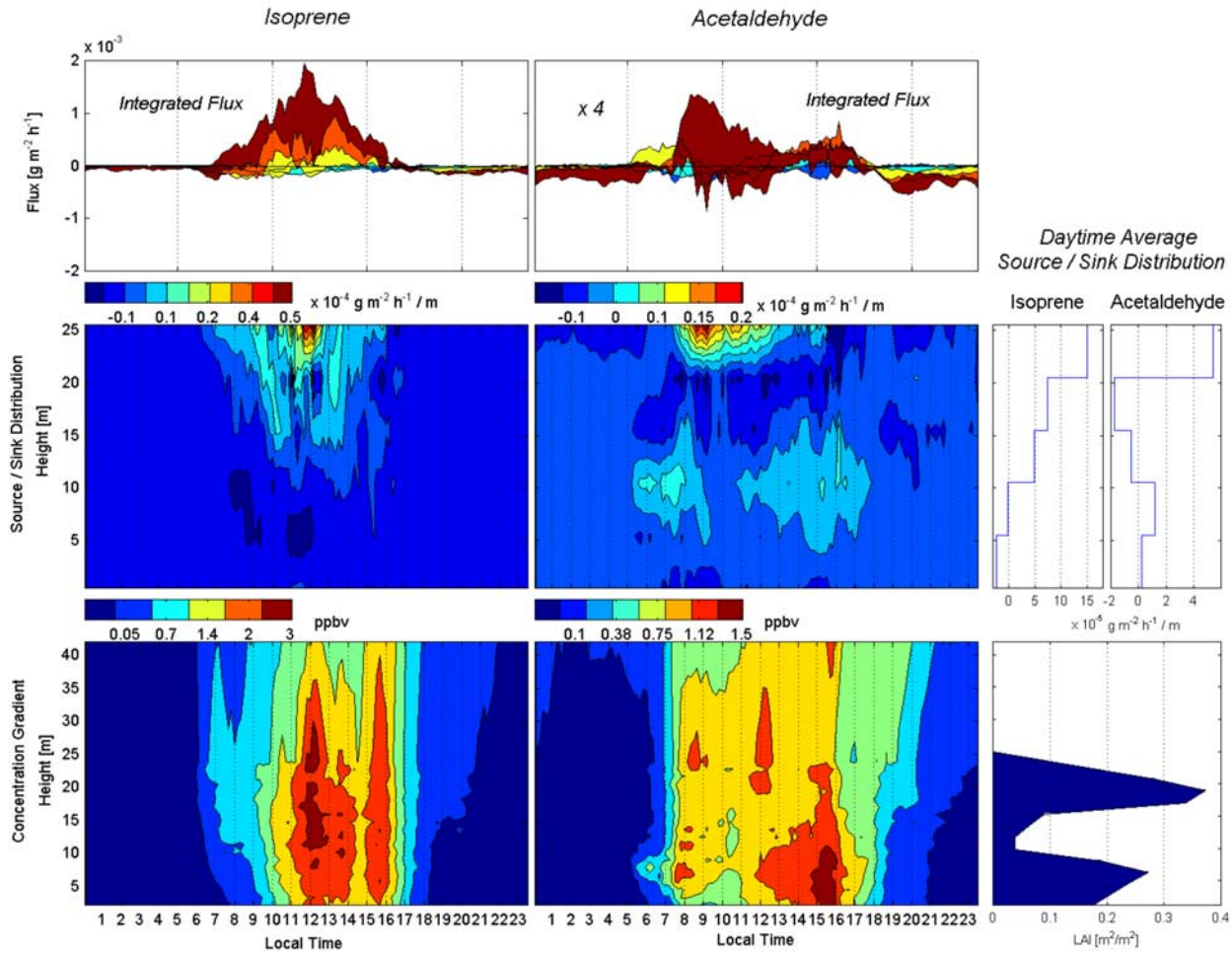

Figure 5. (bottom left and center) Averaged contour plots of isoprene and acetaldehyde concentrations as a function of local time (*x* axis) and height above ground (*y* axis). (bottom right) Measured leaf area index (LAI). (middle left and center) Calculated source/sink distribution of isoprene and acetaldehyde as a function of local time (*x* axis) and height above ground (*y* axis). (middle right) Averaged source/sink distribution during the day. (top) Total fluxes integrated over individual source/sink layers; the color-coding indicates the relative difference between subsequent source/sink layers, and the dark red color represents the top layer.

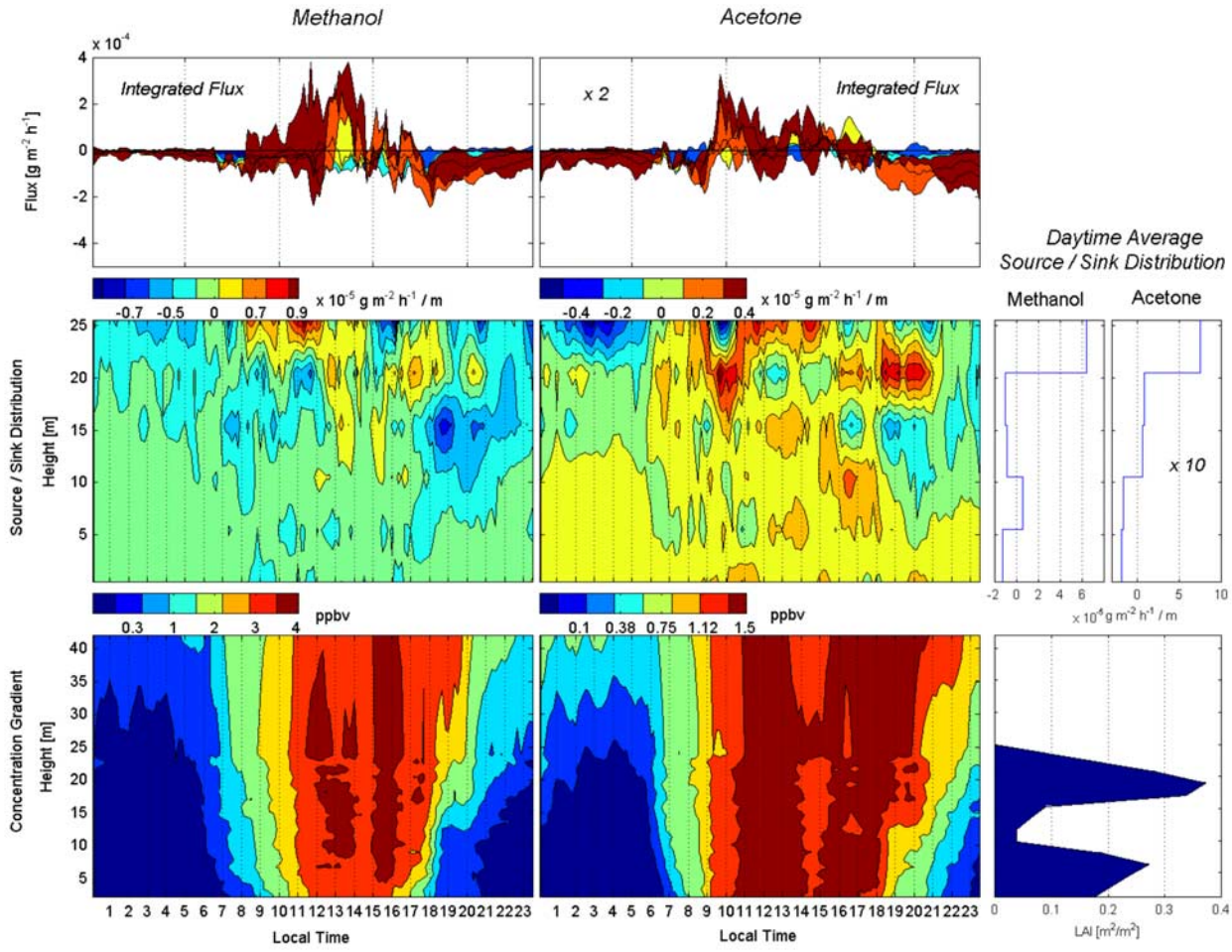

Figure 6. Same as Figure 5 for methanol and acetone.

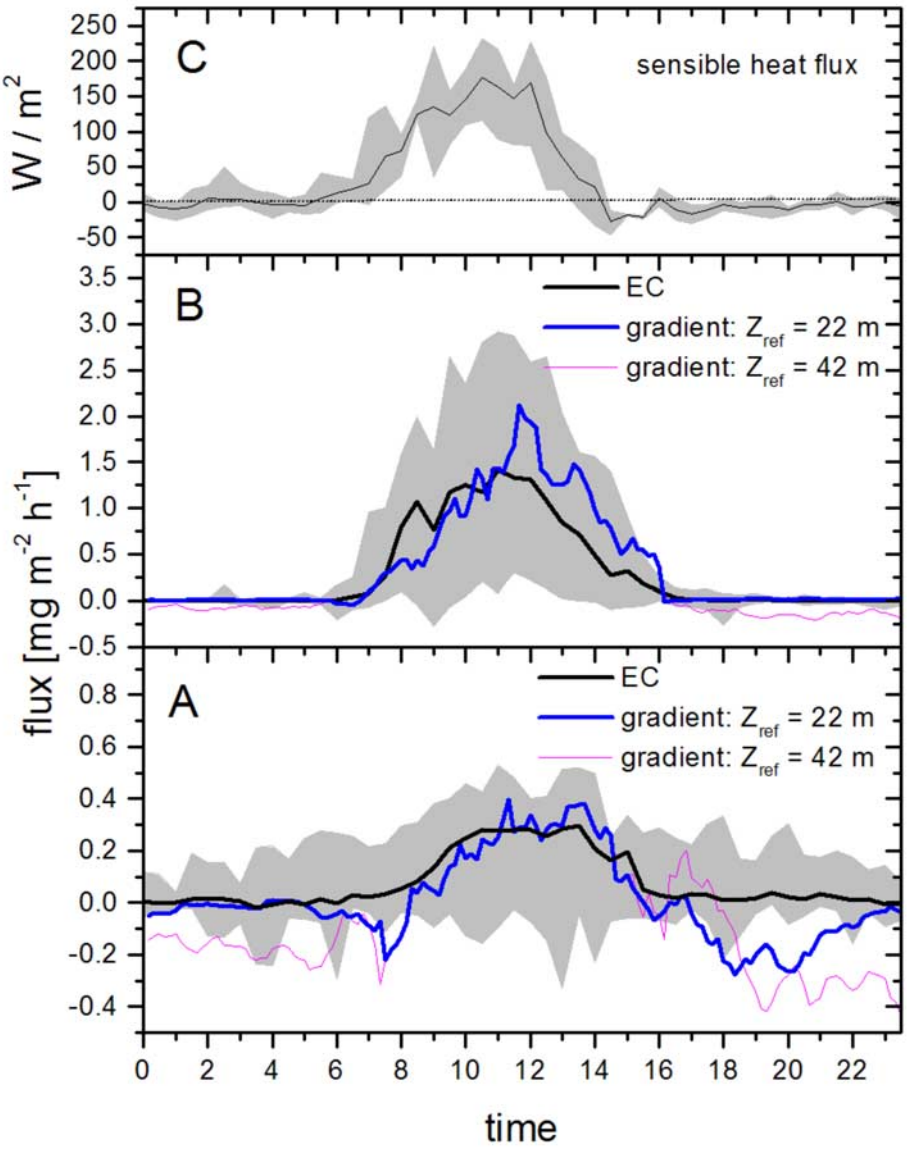

Figure 7. (a) Comparison between the flux obtained by disjunct eddy covariance (black) and the ILT model (blue) for methanol. The pink line illustrates the offset of the ILT model due to a reference height (42 m) above the inversion layer during night; (b) same plot for isoprene; (c) average diurnal cycle of the sensible heat flux during the whole study (dashed line marks zero). The gray area illustrates the range of fluxes observed during the whole campaign.

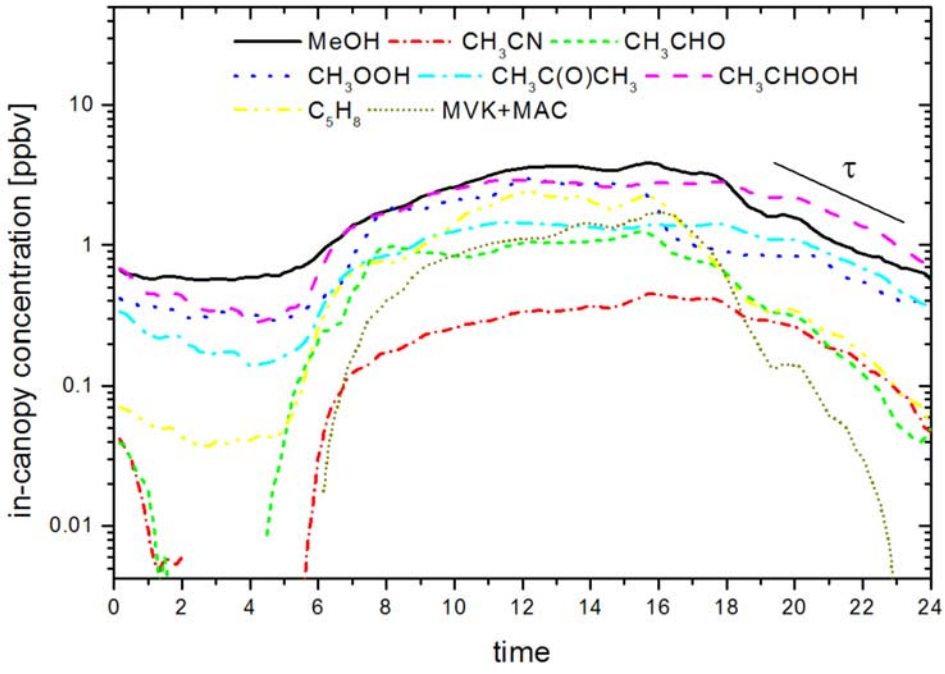

Figure 8. Average diurnal cycle of VOCs within the canopy obtained from the gradient measurements on 4 days during the study.

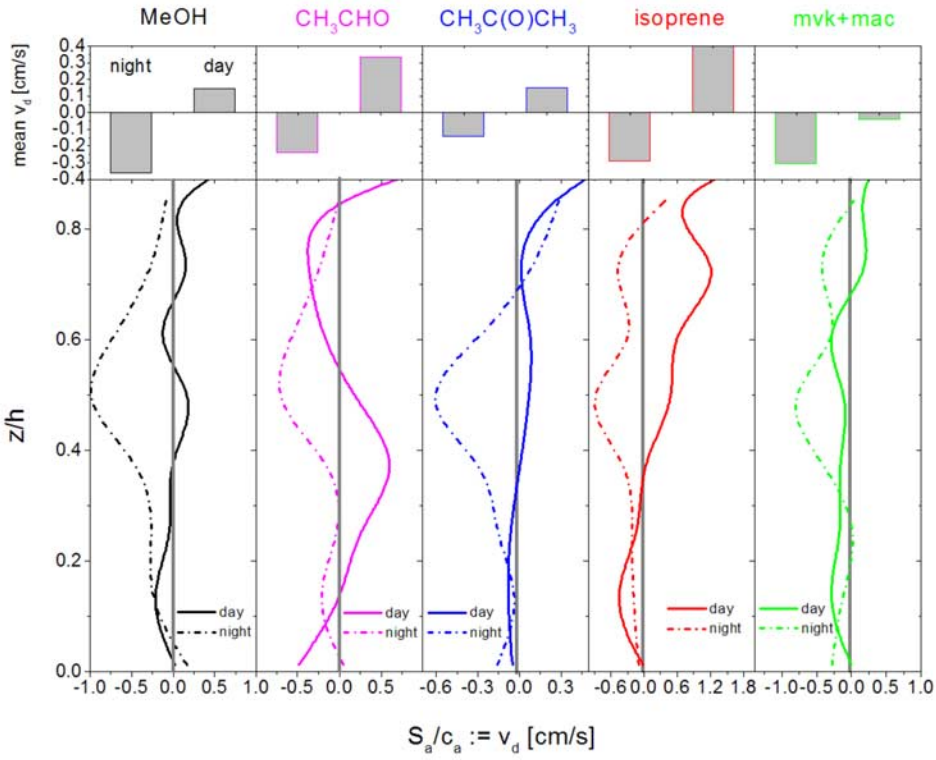

Figure 9. Source/sink layers, expressed as a flux rate (vd: = S_a/c_a), for methanol, acetaldehyde, acetone, isoprene, and MVK+MAC obtained from the dispersion calculation are plotted versus normalized height (z/h) and averaged over day (solid line) and night (dashed line). The top panels depict mean values for day and night.